A walk in the maze: Variation in Late Jurassic tridactyl dinosaur tracks from the Swiss Jura Mountains (NW Switzerland)

Diego Castanera Corresp., [1], **Matteo Belvedere** [2], **Daniel Marty** [2], **Géraldine Paratte** [2], **Marielle Lapaire-Cattin** [2], **Christel Lovis** [2], **Christian A Meyer** [3]

[1] GeoBioCenter, Ludwig-Maximilians-Universität, Bayerische Staatssammlung für Paläontologie und Geologie, Munich, Germany

[2] Section d'archéologie et paléontologie, Paléontologie A16, Office de la culture,, Porrentruy, Switzerland

[3] Department of Environmental Sciences, University of Basel, Basel, Switzerland

Corresponding Author: Diego Castanera
Email address: dcastanera@unizar.es

Background. Minute to medium-sized (FL less than 30 cm) tridactyl dinosaur tracks are the most abundant in the Late Jurassic tracksites of Highway A16 (Reuchenette Formation, Kimmeridgian) in the Jura Mountains (NW Switzerland). During excavations, two morphotypes, one gracile and one robust, were identified in the field. Furthermore, two large-sized theropod ichnospecies (*Megalosauripus transjuranicus* and *Jurabrontes curtedulensis*) and an ornithopod-like morphotype (Morphotype II) have recently been described at these sites. **Methods.** The quality of morphological preservation (preservation grade), the depth of the footprint, the shape variation and the footprint proportions (FL/FW ratio and mesaxony) along the trackways have been analysed using 3D models and false-colour depth maps in order to determine the exact number of small to medium-sized morphotypes present in the tracksites. **Results.** The study of footprints (n = 93) recovered during the excavations has made it possible to identify and characterize the two morphotypes distinguished in the field. The gracile morphotype is mainly characterized by a high footprint length/width ratio , high mesaxony, low divarication angles and clear, sharp claw marks and phalangeal pads (2-3-4). By contrast, the robust morphotype is characterized by a lower footprint length/width ratio, weaker mesaxony, slightly higher divarication angles and clear, sharp claw marks (when preserved), whereas the phalangeal pads are not clearly preserved although they might be present. **Discussion.** The analysis does not allow the two morphotypes to be associated within the same morphological continuum. Thus, they cannot be extramorphological variations of similar tracks produced by a single trackmaker. Comparison of the two morphotypes with the larger morphotypes described in the formation (*Megalosauripus transjuranicus*, *Jurabrontes curtedulensis* and Morphotype II) and the spatio-temporal relationships of the trackways suggest that the smaller morphotypes cannot reliably be considered as small

individuals of any of the larger morphotypes. The morphometric data of some specimens of the robust morphotype (even lower values for the length/width ratio and mesaxony) suggest that more than one ichnotaxon might be represented within the robust morphotype. The features of the gracile morphotype (cf. *Kalohipus* isp.) are typical of "grallatorid" ichnotaxa with low mesaxony whereas those of the robust morphotype (cf. *Therangospodus* isp. and *Therangospodus*? isp.) are reminiscent of *Therangospodus pandemicus*. This work sheds new light on combining an analysis of variations in footprint morphology through 3D models and false-colour depth maps, with the study of possible ontogenetic variations and the identification of small-sized tridactyl ichnotaxa for the description of new dinosaur tracks.

A walk in the maze: Variation in Late Jurassic tridactyl dinosaur tracks from the Swiss Jura Mountains (NW Switzerland)

Diego Castanera[1], Matteo Belvedere[2], Daniel Marty[2], Géraldine Paratte[2], Marielle Lapaire-Cattin[2], Christel Lovis[2], Christian A. Meyer[3]

[1]Bayerische Staatssammlung für Paläontologie und Geologie and GeoBioCenter, Ludwig-Maximilians-Universität Munich, Munich, Germany

[2]Office de la culture, Section d'archéologie et paléontologie, Paléontologie A16, Porrentruy, Switzerland.

[3]Department of Environmental Sciences, University of Basel, Basel, Switzerland

Corresponding author: Diego Castanera

Email address: dcastanera@hotmail.es; d.castanera@lrz.uni-muenchen.de

ABSTRACT

Background. Minute to medium-sized (FL less than 30 cm) tridactyl dinosaur tracks are the most abundant in the Late Jurassic tracksites of Highway A16 (Reuchenette Formation, Kimmeridgian) in the Jura Mountains (NW Switzerland). During excavations, two morphotypes, one gracile and one robust, were identified in the field. Furthermore, two large-sized theropod ichnospecies (*Megalosauripus transjuranicus* and *Jurabrontes curtedulensis*) and an ornithopod-like morphotype (Morphotype II) have recently been described at these sites.

Methods. The quality of morphological preservation (preservation grade), the depth of the footprint, the shape variation and the footprint proportions (FL/FW ratio and mesaxony) along the trackways have been analysed using 3D models and false-colour depth maps in order to determine the exact number of small to medium-sized morphotypes present in the tracksites.

Results. The study of footprints (n = 93) recovered during the excavations has made it possible to identify and characterize the two morphotypes distinguished in the field. The gracile morphotype is mainly characterized by a high footprint length/width ratio, high mesaxony, low divarication angles and clear, sharp claw marks and phalangeal pads (2-3-4). By contrast, the robust morphotype is characterized by a lower footprint length/width ratio, weaker mesaxony, slightly higher divarication angles and clear, sharp claw marks (when preserved), whereas the phalangeal pads are not clearly preserved although they might be present.

Discussion. The analysis does not allow the two morphotypes to be associated within the same morphological continuum. Thus, they cannot be extramorphological variations of similar tracks produced by a single trackmaker. Comparison of the two morphotypes with the larger morphotypes described in the formation (*Megalosauripus transjuranicus*, *Jurabrontes curtedulensis* and Morphotype II) and the spatio-temporal relationships of the trackways suggest that the smaller morphotypes cannot reliably be considered as small individuals of any of the larger morphotypes. The morphometric data of some specimens of the robust morphotype (even lower values for the length/width ratio and mesaxony) suggest that more than one ichnotaxon might be represented within the robust morphotype. The features of the gracile morphotype (cf. *Kalohipus* isp.) are typical of "grallatorid" ichnotaxa with low mesaxony whereas those of the robust morphotype (cf. *Therangospodus* isp. and *Therangospodus*? isp.) are reminiscent of *Therangospodus pandemicus*. This work sheds new light on combining an analysis of variations in footprint morphology through 3D models and false-colour depth maps, with the study of possible ontogenetic variations and the identification of small-sized tridactyl ichnotaxa for the description of new dinosaur tracks.

64

65 INTRODUCTION

66 Since the first sauropod tracks were reported in the Lommiswil quarry (Late Kimmeridgian,
67 Canton Solothurn) in the Swiss Jura Mountains (Meyer, 1990), dinosaur track discoveries have
68 increased considerably, and to date more than 25 tracksites have been documented in the cantons
69 of Jura, Bern, Neuchâtel and Solothurn. Most of these tracksites occur in the Reuchenette
70 Formation (Kimmeridgian), and some of them in the Twannbach Formation (Tithonian) (Meyer
71 & Thüring, 2003; Marty, 2008; Marty & Meyer, 2012; Marty et al., 2010; 2013). Between 2002
72 and 2011, six large tracksites were systematically excavated and documented by the
73 Palaeontology A16 (Marty and Billon-Bruyat, 2009) prior to the construction of Highway A16 in
74 the Canton Jura (NW Switzerland). These tracksites covered together a surface area of 18,500
75 m^2, and a total of 59 ichnoassemblages. Out of 14,000 individual tracks, 254 trackways were
76 attributed to sauropods and 411 to bipedal tridactyl dinosaurs. Therefore, the Jura carbonate
77 platform has today become a key area for Late Jurassic dinosaur palaeoichnology (Marty, 2008;
78 Marty & Meyer, 2012) as it represents one of the areas with the highest number of Late Jurassic
79 dinosaur tracks in the world.

80 Recent papers have described giant theropod tracks (*Jurabrontes curtedulensis*, Marty et al.,
81 2017) and large theropod tracks (*Megalosauripus transjuranicus*, Razzolini et al., 2017) from the
82 Swiss Jura Mountains, but most of the tridactyl tracks by far are the still largely undescribed
83 minute, small and medium-sized tracks (footprint length < 30 cm). Marty (2008) described
84 minute and small tridactyl tracks from the Chevenez—Combe Ronde tracksite (Canton Jura, NW
85 Switzerland) and tentatively attributed some of these to *Carmelopodus*. Since then, however,
86 many other tracksites and ichnoassemblages with minute to medium-sized tridactyl tracks have
87 been discovered, including some very well-preserved tracks of different morphotypes and some
88 very long trackways (up to 100 m).

89 In Europe, apart from the Swiss and French (Mazin, Hantzpergue & Pouech, 2016) Jura
90 Mountains, the main Late Jurassic deposits that have yielded minute to medium-sized tridactyl
91 dinosaur tracks are located in the Lusitanian Basin in Portugal (Antunes & Mateus, 2003; Santos,
92 2008), the Asturian Basin in Spain (Lockley et al., 2008; Piñuela, 2015), the Aquitanian Basin in
93 France (Lange-Badré et al., 1996; Mazin et al., 1997; Moreau et al., 2017), the Lower Saxony
94 Basin in NW Germany (Kaever & Lapparent, 1974; Diedrich, 2011; Lallensack et al., 2015), and
95 several units in the Holy Cross Mountains in Poland (Gierliński, Niedźwiedzki & Nowacki,
96 2009). The units that date to around the Jurassic-Cretaceous boundary (Tithonian–Berriasian) in
97 the Iberian Range in Spain (Santisteban et al., 2003; Castanera et al., 2013a; Alcalá et al., 2014;
98 Campos-Soto et al., 2017) should also be mentioned. It is noteworthy that, while there is a high
99 number of small to medium-sized tridactyl tracks (assigned to both theropods and ornithopods)
100 described, only few ichnotaxa have been formally erected so far. Besides the tracks from the
101 Chevenez—Combe Ronde tracksite tentatively assigned to *Carmelopodus* by Marty (2008), the

main small to medium-sized tridactyl tracks identified have been from Spain (*Grallator* and *Anomoepus,* from several sites in Asturias, Lockley et al., 2008; Piñuela, 2015; Castanera, Piñuela & García-Ramos, 2016), France (*Carmelopodus*, Loulle tracksite, Mazin, Hantzpergue & Pouech, 2016), Poland (*Wildeichnus*, cf. *Jialingpus* and *Dineichnus*, different units in the Holy Cross Mountains, Gierliński, Niedźwiedzki & Nowacki, 2009), Germany (*Grallator*, Bergkirchen tracksite, Diedrich, 2011) and Portugal (*Dineichnus* and ?*Therangospodus*, Lockley et al., 1998a; Lockley, Meyer & Moratalla, 2000). Other significant Late Jurassic areas with minute to medium-sized tridactyl dinosaur tracks are found in the USA (Foster & Lockley, 2006), Morocco (Belvedere, Mietto & Ishigaki, 2010), China (Xing, Harris & Gierliński, 2011; Xing et al., 2016), Yemen (Schulp & Al-Wosabi, 2012) and Turkmenistan (Lockley, Meyer & Santos, 2000; Fanti et al., 2013).

Several recent papers have examined the variability in track morphology along trackways (Razzolini et al., 2014, 2017; Lallensack, van Heteren, & Wings, 2016), showing how pronounced changes can occur along a single trackway. Thus, sometimes it can be very difficult to determine the exact number of ichnotaxa and clearly distinguish between them, especially when the tracks are morphologically similar. This should be borne in mind particularly when studying the material from Switzerland, where large theropod tracks have shown notable variations in shape along the same trackway (Razzolini et al., 2017). In the case of the minute to medium-sized tridactyl tracks, two different morphotypes were identified at first glance during the documentation of the tracksites, one gracile and one more robust type. The aim of this paper is to describe the small to medium-sized tridactyl tracks collected in the Jura Mountains (NW Switzerland). Special emphasis is put on the analysis of track morphology through 3D models and possible variations in footprint shape along trackways in order to find out if the different morphotypes are a consequence of preservation. In addition, other factors such as possible ontogenetic variations in the larger ichnospecies described in the formation are also taken into account. Finally, we discuss the ichnotaxonomy of the tracks.

GEOGRAPHICAL AND GEOLOGICAL SETTING

The studied material comes from six different tracksites from Highway A16 and nearby areas (Fig. 1A): (1) Courtedoux—Bois de Sylleux (CTD–BSY), (2) Courtedoux—Tchâfouè (CTD–TCH), (3) Courtedoux—Béchat Bovais (CTD–BEB), (4) Courtedoux—Sur Combe Ronde (CTD–SCR), (5) Chevenez—Combe Ronde (CHE–CRO); and (6) Chevenez—La Combe (CHE–CHV). For the sake of simplicity BSY, TCH, BEB, SCR, CRO and CHV are used in the publication.

All the tracksites are located in the Ajoie district about 6-8 km to the west of Porrentruy (Canton Jura, NW Switzerland) on the track of Swiss federal highway A16 except the Chevenez—La Combe tracksite, which is located in a quarry near the village of Chevenez. The first five

tracksites were systematically excavated level-by-level by the Palaeontology A16 (PALA16) from 2002 until 2011 (Marty et al., 2003; Marty et al., 2004; Marty et al., 2007; Marty, 2008; Marty and Billon-Bruyat, 2009).

Geologically, the study area belongs to the Tabular Jura Mountains and is located at the eastern end of the Rhine-Bresse transfer zone between the Folded Jura Mountains (South and East) and the Upper Rhine Graben and Vosges Mountains (North). The Upper Jurassic strata of the Swiss Jura Mountains are made up of shallow-marine carbonates deposited on the large and structurally complex Jura carbonate platform, which was located at the northern margin of the Tethys at a palaeolatitude of approximately 30° N (Thierry, 2000; Thierry et al., 2000; Stampfli & Borel, 2002).

The tracksites occur within the Reuchenette Formation (Kimmeridgian), dated by ammonites of the Cymodoce to Mutabilis (Boreal), and Divisum to Acanthicum (Tethyan) biozones (Comment et al., 2015). Accordingly, the age of the track-bearing levels is late Early to early Late Kimmeridgian (Gygi, 2000; Jank et al. 2006). This age is also confirmed by the presence of ostracods (Schudack et al., 2013). More information on the sedimentology and palaeoenvironment of the Highway A16 tracksites can be found in Jank et al. (2006), Marty (2008), Razzolini et al. (2017) and Marty et al. (2017).

Stratigraphically, the tracksites include three different track-bearing laminite intervals, separated by shallow marine limestones (Marty, 2008; Waite et al., 2008; Comment, Ayer & Becker, 2011; Comment et al., 2015). The three main track-bearing laminite intervals are referred to as the lower, intermediate and upper levels, respectively levels 500–550, 1000–1100, and 1500–1650 (Fig. 1B). Only tracks from the lower and intermediate track levels are included in the present study (Fig. 1B), and the studied tracks come from a total of 11 different ichnoassemblages (stratigraphic track levels). These are as follows: BEB500, CRO500, BSY1020, BSY1040, BSY1050, TCH1055, SCR1055, TCH1060, TCH1065, TCH1069 and CHV1000–1100 (precise level cannot be indicated).

MATERIAL AND METHODS

We analysed a total of 93 individual tracks (Table S1) that are housed in the track collection of PAL A16 (Canton Jura), either as original specimens or as replicas. This collection will be transferred to JURASSICA Muséum (Porrentruy, Canton Jura) in 2019. All the tracks are from the aforementioned tracksites, the largest samples coming from BEB500 (39 footprints), TCH1065 (15) and CRO500 (20). Each analysed track has two acronyms (Table S1): one represents the number of the slab within the collection, e.g.: TCH006-1100 denotes Tchâfouè tracksite, year 2006 (the year of discovery), slab 1100 (an “r” in front of the specimen number, means replica). Some high-resolution laser scans were made in the field and those tracks are here referred to as “Laser-Scan”. A second acronym represents the level and number of the trackway

and track, e.g.: TCH1055-T2-L1 denotes Tchâfouè tracksite, level 1055, trackway 2, track 1, left pes. The second acronym is used throughout the manuscript. As the track-bearing layers were excavated level-by-level there are no doubts about the preservation mode of the tracks. Thus, all the tracks were preserved as true tracks (concave epireliefs) and were produced on the tracking surface, with the only exception of TCH1060-E58, which was preserved as a natural cast (convex hyporelief).

Analysis of track morphology was performed independently for each track; however, some tracks belong to trackways, therefore their variation in morphology along a single trackway was also considered in order to avoid over-identification of morphotypes. These trackways are: BEB500-T16 (3), BEB500-T17 (4), BEB500-T58 (6), BEB500-T73 (4), BEB500-T75 (2), BEB500-T78 (2), BEB-500-T82 (2), BEB-500-T93 (2), BEB500-T120 (4), CRO500-T10 (14), CRO500-T30BIS (5), TCH1055-T2 (2), TCH1065-T15 (2), TCH1065-T25 (2) and TCH1069-T2 (2). We analysed each individual track and made an evaluation of the quality of preservation according to the scale of Belvedere and Farlow (2016) (Table S1). As stated by these authors, "quantitative shape analyses need to be based on data of high quality, and comparisons are best made between tracks comparable in quality of preservation". Accordingly, only the tracks with a preservation grade equal to or higher than 2 were considered for measurement and analysed in this paper; field measurements exist for all the other tracks and are stored in the PALA16 database. The descriptions are based on identification of two different morphotypes, one gracile and one robust, during the documentation in the field. Thus, the footprint length (FL), footprint width (FW), length and width of digits II (LII, WII), III (LIII, WIII) and IV (LIV, WIV), divarication angles (II-III; III-IV) were measured (see Castanera, Piñuela & García-Ramos, 2016, fig. 2). Subsequently, the FL/FW ratio and the mesaxony were calculated. The latter was calculated on the basis of the anterior triangle length–width ratio (AT) following Lockley (2009). All these measurements were taken from perpendicular pictures with the software Image J. The tracks were classified according to different size classes (Marty, 2008) on the basis of pes length (FL) as: 1) minute, FL < 10 cm; 2) small, 10 cm < FL < 20 cm; 3) medium, 20 cm < FL < 30 cm; and 4) large, FL > 30 cm. The morphometric data of the studied tracks were compared in a bivariate plot (length/width ratio vs. mesaxony) with larger tracks (*Megalosauripus transjuranicus*, *Jurabrontes curtedulensis* and Morphotype II) described in the Reuchenette Formation (Razzolini et al., 2017; Marty et al., 2017). In addition, they were also compared with other theropod ichnotaxa using data from Castanera, Piñuela & García-Ramos (2016) which were mainly compiled after Lockley (2009) and Xing et al. (2014). Data were analysed with the software PAST v.2.14 (Hammer, Harper & Ryan, 2001).

3D-photogrammetric models were generated from pictures taken with a Canon EOS 70D camera equipped with a Canon 10-18mm STL lens using Agisoft Photoscan (v. 1.3.2, www.agisoft.com) following the procedures of Mallison & Wings (2014) and Matthews, Noble & Breithaupt (2016). Within the BEB500 sample, 3D data of 10 footprints were obtained by high-resolution laser-scanning carried out in the field in 2011 by Pöyry AG with a Faro hand-scanner. Most of

these 10 footprints were destroyed during the construction of Highway A16. The scaled meshes were exported as Stanford PLY files (.ply) and then processed in CloudCompare (v.2.7.0, www.cloudcompare.com) in order to obtain accurate false-colour depth maps. All photogrammetric meshes used in this study are available for download here: https://doi.org/10.6084/m9.figshare.5662306 (ca. 2.5 Gb). In addition, we analysed the maximum depth of all the tracks, in order to ascertain whether there is a relationship between depth, preservation grade and the morphotype. The maximum depth was estimated using the false-colour map derived from the 3D-model in those tracks with a preservation grade generally higher than 0.5.

DESCRIPTION OF THE TRACK MORPHOTYPES AND MORPHOLOGICAL VARIATIONS ALONG THE TRACKWAYS:

Gracile morphotype:

This morphotype was identified in all six tracksites. The footprints are small to medium-sized (15-21.2 cm) tridactyl tracks (Fig. 2), clearly longer than wide (FL/FW ratio = 1.50-1.90) (Table 1). The digits are slender with an acuminate end and clear claw marks preserved in the three digits in the majority of the tracks. Digit III is clearly longer and slightly wider than digits II and IV. Digits II and IV are similar in length and width. The mesaxony is variable but medium to high (AT =0.53-0.98), with a mean value of 0.77, although it is higher in most of the specimens (more than 0.8 in half of the sample). The divarication angles are relatively low, II-III generally being slightly higher (mean 25º) than III-IV (mean 22º). The hypices are quite symmetrical. The "heel" morphology is variable; some specimens have an oval to round heel pad connected with digit IV (BEB500-T16-R3, TCH1055-E53, TCH1055-T2-R1, TCH1069-T1-R2; see Fig. 2), whereas in others it is not clearly preserved even when the preservation grade is high (e.g.: BSY1020-E2). Most of the specimens preserve a clear small medial notch located behind digit II, which with the rounded heel marks gives them an asymmetric shape. In some of the footprints well-defined digital pads can be discerned. The tracks with the best quality of preservation suggest a phalangeal formula of 2-3-4 (including the metatarsophalangeal pad IV).

Robust morphotype:

This morphotype has mainly been identified on the track levels BEB500 and TCH1065. The footprints are small or medium-sized (17-21.8 cm) tridactyl tracks (Fig. 3), slightly longer than wide (FL/FW ratio = 1.13-1.46), (Table 1). The digits are relatively robust with an acuminate end and clear claw marks preserved in some of the tracks (e.g.: BEB500-T120-R5, TCH1065-T15-R1, TCH1065-T21-R1). Digit III is clearly longer and slightly wider than digits II and IV. Digits II and IV are similar in length and width. The mesaxony is variable but low-medium (AT =0.38-0.61), with a mean value of 0.49. The divarication angles are low, II-III (mean 26º) and III-IV (mean 27º) being quite similar. The hypices are quite symmetrical. The "heel" morphology is variable, ranging from subrounded to subtriangular. Only TCH1065-T21-R1

preserves a clear small medial notch located behind digit II, thus being slightly asymmetrical, whereas the other specimens are more symmetrical. Well-defined digital pads cannot be discerned in most of the footprints, although TCH1065-T21-R1 shows digital pads suggesting a possible phalangeal pad formula of 2-3-?4.

Table 2 and Figs. 4 and 5 show the variations in preservation grade and the maximum depth along the analysed trackways (see Table S1 to see the data of each specific track). 11 trackways belong to the gracile morphotype and 4 trackways belong to the robust morphotype (see Figs. S1-S3 for the location of the trackways in the tracksite). The preservation grade varies from low (0-0.5 in the scale) to high (2 or more in the scale) for both morphotypes. The maximum depth variation is considerably low, as the maximum variation it is around 5 mm in both morphotypes (CRO500-T30BIS and BEB500-T120),

DISCUSSION:

1) True ichnodiversity or variation due to substrate-foot interaction?

The final shape of a footprint is determined by a combination of factors related to the anatomy of the trackmaker's autopodium, the kinematics and the substrate (Marty et al., 2009; Falkhingham, 2014); another important factor is the level in which the tracks were preserved (Milàn & Bromley, 2006) , i.e. if they are preserved as undertracks. In the case of the tracksites of Highway A16, we can rule out this factor as the excavations were carried out level-by-level, so the footprints are true tracks (or natural casts). As the foot-substrate interaction is a major determinant of the final shape of a track, it is important to analyse variations in depth and shape along trackways to ascertain the morphological variation (e.g.: Razzolini et al., 2014). For this reason, we first analysed the individual footprint shape (Figs. 2, 3) and then looked at the variation along the trackway (Figs. 4, 5). The idea was to establish whether some of the described morphotypes might represent variations produced by the same/similar trackmakers (in the sense of a theropod with tridactyl functionally similar pes structure, as it is not possible to assign the tracks to a particular clade) walking on a substrate with different properties (water content, thickness or cohesiveness). Previous researchers have described variations in dinosaur footprint shape between two extremes of a morphological continuum or a gradational series (Gatesy et al., 1999; Razzolini et al., 2014) to suggest that similar theropods traversed substrates of variable consistency. Other researchers have shown variations in dinosaur footprint morphology as a consequence of locomotor adaptations associated with changes in substrate consistency (Wilson et al., 2009). Thus, the same trackmaker can produce footprints with significant shape variation along the trackways when there is a change in the aforementioned substrate properties. Only in such cases where the analysis is along the trackway, the differences can be claimed as a consequence of foot-substrate interactions rather than anatomical differences in the foot morphology of the trackmaker. In the Swiss samples, clear evidence of intermediate morphologies is missing, supporting the presence of at least two different groups of tridactyl

trackmakers. Where gradational series of theropod tracks have been reported (see refs above), these show a hallux, metatarsal marks, and distinctive displacement rims in the deepest tracks that are clearly extramorphological features. None of the morphotypes presented in this paper shows such evidence, even in the deepest tracks. This leads us to think that the sediment was relatively firm during the production of the tracks.

Generally, tracks with a preservation grade of 1 or higher can be classified in one of the two described morphotypes: gracile or robust. There are just a few classification doubts regarding isolated footprints (e.g.: CRO500-T30BIS-R4). At the outset, one possible hypothesis was that the robust morphotype could be a variation of the gracile morphotype, produced by a similar trackmaker on a substrate with different rheological properties (e.g.: Gatesy et al., 1999; Razzolini et al., 2014). This hypothesis was especially appealing given the similar footprint dimensions of the two morphotypes. Thus, the deeper tracks would look more robust than the shallow ones, and the absence of clear phalangeal pad marks in most of the robust morphotype tracks might be a consequence of a softer substrate or of deeper penetration by the trackmaker foot. Our max-depth analysis (see Tables 2 and S1), indeed showed that the robust tracks have high values of maximum depth (e.g.: BEB500-T120-R5 = 6.1 mm; BEB500-T120-R6 = 10 mm; BEB500-E1 = 10.5 mm; TCH1065-E124 = 6.9 mm; TCH1065-E188 = 5.9 mm; TCH1065-T15-R1 = 8.3 mm; TCH1065-T21-R1 = 12.1 mm, see Table S1). However, it is worth noticing that the highest values all occur on level TCH1065, where also the gracile tracks show their deeper values (TCH1065-E28 = 11.7 mm; TCH1065-T25-R2 = 12.9 mm; TCH1065-T25-L2 = 10.2 mm), quite comparable to the robust ones. Therefore, on this track level the presence of the two morphotypes cannot be directly associated with the depth of the footprints, as both the gracile and the robust show similar values of maximum depth. In the case of BEB500 we see a similar scenario, e.g., BEB500-T16 and BEB500-T17 (gracile) have the same depth as BEB500-T120 and BEB500-E1 (robust). In other words, the depth of the tracks is more determined by the level where they were impressed than by being robust or gracile. Anyway, it is noteworthy that the max-depth analysis shows that depth values are relatively low with maximum depths of slightly more than just 1 cm in the deepest tracks.

The analysis of the morphological variation along the trackways shows that the gracile morphotype is quite consistent along the trackways, and no tracks classifiable as robust are found within these trackways. There are only a few cases, e.g. CRO500-T30BIS-R4 (Fig. 5B) and BEB500-T17-L8/ BEB500-T17-L9 (Fig. 4B), which might look more robust than the other tracks in the trackway, but here the features did not properly fit with the description of the robust morphotype. Regarding the robust morphotype, in the analysed trackways (BEB500-T120, TCH1065-T15 and TCH1069-T2) none of the tracks shows any feature of the gracile morphotype (noteworthy is the low preservation grade and the scarce data for TCH1065-T15 and TCH1069-T2). The maximum variation in depth along the trackways is low, being around 5 mm in both morphotypes (Gracile, CRO500-T30BIS = 4.7 mm; Robust, BEB500-T120 = 5.8 mm). These data suggest that, in our case, there is no clear correlation between the depth of the

footprint and the morphotypes (either gracile or robust), and that the intra-trackway variation is never significant enough to denote a shift between the morphotypes. Therefore, the present evidence indicates that there are *at least* (see following discussion) two different trackmakers of small to medium-sized theropods in the tidal flats of the Jura Mountains.

Analysis of the mesaxony (it represents how far the projection of digit III extends with respect to digits II and IV) and the FL/FW ratio supports the presence of *at least* the two morphotypes (Fig. 6). Some authors have used mesaxony (Weems, 1992; Lockley, 2009) as a good parameter to distinguish between tridactyl tracks. In the studied sample, this parameter is clearly lower in the robust morphotype than in the gracile one. The FL/FW ratio also shows a considerable difference between the morphotypes (likewise lower in the robust morphotype). A closer look at these two parameters within the robust morphotype (Fig. 6B) raises the question whether it represents a single ichnotaxon. The data for the two analysed tracks from BEB500-T120 (AT = 0.38-0.40; FL/FW = 1.13-1.16) show considerably lower data for the FL/FW ratio and weaker mesaxony than the tracks from TCH1065, (AT = 0.52-0.61; FL/FW = 1.23-1.46) (see also following discussion).

2) Morphotype variation due to ontogeny?

Another salient point relating to the number of morphotypes in the analysed sample is the possibility of variations due to different ontogenetic states. Few works have dealt with the relationship between dinosaur footprints and ontogeny (e.g.: Lockley, 1994; Matsukawa, Lockley & Hunt, 1999; Hornung et al., 2016). Ontogenetic variations have been suggested to explain morphological variation in the classical theropod ichnotaxa of the *Grallator-Eubrontes* plexus (Olsen, 1980; Olsen, Smith & McDonald, 1998; Moreau et al., 2012). Olsen, Smith & McDonald, (1998) proposed that the major proportional differences between *Grallator*, *Anchisauripus* and *Eubrontes* might be derived from the allometric growth of individuals of several related species. In these typical theropod footprints the large tracks (*Eubrontes*) are wider with weaker mesaxony than the smaller tracks (*Grallator*), showing a positive correlation between the elongation of the track and the elongation of the anterior triangle (Lockley, 2009). As this author suggested, the assumption of ontogenetic variation is thus based mainly on the assumption of a discernible allometric pattern. Although the growth dynamics have been documented in several groups of theropods (Bybee et al., 2006; Griffin, 2018 and references therein) little is known about how possible ontogenetic variations may have affected variations in theropod feet proportions and thus in footprint shape (Farlow and Lockley, 1993; Farlow et al., 2013). Generally tracks that are similar in morphology but different in size are considered to belong to the same ichnotaxon (Thulborn, 1990; Lockley, 1994; Matsukawa, Lockley & Hunt, 1999; Clark, Ross & Booth, 2005; Pascual-Arribas & Hernández-Medrano, 2011; Castanera et al., 2015). Demathieu (1990) also explored the use of ratios of length characters to reduce the influence of size when comparing footprints. For instance, Lockley, Mitchel & Odier (2007) assumed that small theropod tracks (*Carmelopodus*) from the Jurassic of North America represent adults of small species and not juveniles of larger species and suggested that “this

inference is consistent with a model of rapid growth rates such as is typical of birds, which would have reduced the number of potential track making juveniles that could habitually make footprints". By contrast, Pascual Arribas and Hernández-Medrano (2011) considered minute theropod tracks from the Early Cretaceous of Spain (subsequently assigned to *Kalohipus bretunensis* by Castanera et al., 2015) to belong to baby theropods because of the morphometric similarities with larger tracks from the same site and formation.

Two possible different ontogenetic stages should be considered in the interpretation of the Ajoie ichnocoenosis. In one case, there are similarities between the gracile morphotype and the previously described *Carmelopodus* tracks from the Chevenez-Combe Ronde tracksite (CRO500-T8; CRO500-T10; CRO500-T16; CRO500-T21; CRO500-T26; CRO500-T41) so the first hypothesis would be that both are an ontogenetic variation of the same morphotype. According to the original description by Marty (2008), these tracks can be characterized as mesaxonic, slightly asymmetric, tridactyl tracks that are clearly longer than wide. Digit III is always the longest, digit IV being longer than digit II, which is shorter posteriorly. Claw impressions are present in the three digits, and there is a phalangeal pad formula of 2-3-3. There is a low total divarication angle, and divarication angles of the same order between digits II and III, and III and IV. It has a narrow-gauge trackway with small tracks with outward rotation. CRO500-T10-L10 is the track with the highest preservation grade recovered from level CRO500. Regarding the data taken from this footprint, it should be noted that the FL/FW ratio (1.69) falls within the range of the other gracile tracks, while the mesaxony is among the highest in the whole sample (0.96) but still within the range of the gracile morphotype (Fig. 6). The divarication angle is also low (32º-23º). Moreover, reanalysis of the tracks with the use of false-colour depth maps (Fig. 2F) allowed the fourth phalangeal pad in digit IV to be distinguished, suggesting a formula of 2-3-4, although this is not preserved in most of the tracks with a lower preservation grade (Fig. 5A). Accordingly, we consider that there are not enough data to interpret CRO500-T10-L10 as a different morphotype of the tracks included in the gracile morphotype and we regard them as part of it (see next section for the new ichnotaxonomic assignation). This highlights the importance of analysing large samples and the variation in shape through the trackways. The differences in size between CRO500-T10-L10 (FL = 11 cm) and the rest of the specimens of the gracile morphotype (FL= 16-21.2 cm) but similar footprint shape, FL/FW ratio and mesaxony might be explained by an isometric growth. However, the absence of more data of smaller size classes of the gracile morphotype, prevent us to test this first hypothesis.

A second hypothesis considers whether the gracile and the robust morphotype might be ontogenetic variations of one of the three previously identified larger ichnotaxa (*Megalosauripus transjuranicus, Jurabrontes curtedulensis* and the informally named Morphotype II tracks) of the Jura Mountains (Razzolini et al., 2017; Marty et al., 2017). The two formally described ichnospecies represent large and more slender (*Megalosauripus transjuranicus*) and giant and more robust (*Jurabrontes curtedulensis*) theropod tracks, respectively. In addition, the third large morphotype not assigned to any known ichnotaxon and named Morphotype II is characterized by

subsymmetric tracks that are generally slightly longer than wide (sometimes almost as wide as long), blunt digit impressions, with no evidence for discrete phalangeal pad and claw marks (Razzolini et al., 2017). The interpretation of this morphotype is quite complex, as tracks with the aforementioned features have been also documented as a morphological variation in *Megalosauripus* trackways. However, other trackways show a very consistent morphology throughout very long trackways, and have been considered by the authors a true unnamed ichnotaxon different from *Megalosauripus* and with a probable ornithopod affinity. This means that tracks with Morphotype II features can represent two different trackmakers, a theropod (*Megalosauripus*) and an ornithopod (the proper informally named Morphotype II). Long trackways of Morphotype II are found on the same surfaces that many in the studied sample come from, such as BEB500 and CRO500 (Razzolini et al., 2017). Thus, the hypothesis that the gracile and the robust morphotypes might represent juvenile/subadult specimens of the larger tracks described in the tracksites must be explored.

Analysing footprint proportions, it should be noted that the FL/FW ratio of the gracile morphotype fits within the upper range of the tracks included in the ichnotaxon *Megalosauripus* (Fig. 6A) from the Reuchenette Formation; considering just the type material of *Megalosauripus transjuranicus*, it fits well (Fig. 6B) (Razzolini et al., 2017). However, the mesaxony is substantially higher in the gracile morphotype than in the *Megalosauripus* tracks. In the case of the robust morphotype, the FL/FW ratio fits within the range of *Jurabrontes curtedulensis* and the Morphotype II tracks when analysing all the referred material (Fig. 6A) or just the type material of *Jurabrontes curtedulensis* and the best-preserved tracks of Morphotype II (BEB500-TR7-L2; BEB500-TR7-R2; BEB500-TR7-R7; BEB500-TR7-L10, Razzolini et al., 2017) (Fig. 6B). The robust morphotype has higher mesaxony than *Jurabrontes curtedulensis*, being more similar in this respect to the Morphotype II tracks. It is notable that the footprint proportions within the robust morphotype are quite variable between stratigraphic levels. For example, tracks from trackway BEB500-T120 have a lower FL/FW ratio and mesaxony, whereas tracks from track level TCH1065 have higher ratios. Thus, BEB500-T120 is closer to the ranges of *Jurabrontes curtedulensis* whereas the tracks from TCH1065 are closer to the ranges of *Megalosauripus transjuranicus* and especially the Morphotype II tracks (Fig. 6).

As previously discussed, the variations in mesaxony, where larger tracks have lower mesaxony, are well documented in theropod tracks (Weems, 1992; Olsen, Smith & McDonald, 1998; Lockley, 2009). Because there are some overlapping areas in the footprint proportions of the larger and the smaller tracks, it might be tempting to relate them according to these values; i.e. gracile with *M. transjuranicus*, robust from BEB500 with *Jurabrontes*, and robust from TCH1065 with Morphotype II. Nonetheless, the smaller morphotypes show other considerable morphological differences apart from size and mesaxony with respect to the larger morphotypes. The gracile morphotype differs from *M. transjuranicus* in key features of the diagnosis such as the sigmoidal impression of digit III (less sigmoidal), the divarication angle (less divaricated) and the digital pad of digit IV (proportionally smaller when preserved). The robust morphotype

(from both BEB500 and TCH1065) differs from *Jurabrontes curtedulensis* in the absence of clear phalangeal pads (preservation bias?), the absence of the peculiar, isolated proximal pad PIII1 of digit III, and the interdigital divarication angles (asymmetric vs symmetric); it also differs from the Morphotype II tracks in the absence of blunt digit impressions, possible evidence of a discrete phalangeal pad, and the presence of clear claw marks. Therefore, despite some overlap of the morphometric data and the fact that there are considerable differences in shape (although some of them might be extramorphological variations), we consider that there are not enough data to support the second hypothesis just on the basis of the footprint shape and morphometric data.

Finally, we examine whether there is any spatio-temporal relationship between the larger and the smaller tracks from the Ajoie ichnocoenosis. Lockley (1994) warned that the track data "that most probably represent monospecific assemblages are those obtained for a single ichnotaxon from a single bedding plane". In this regard, it is interesting to note the scarcity of large theropod tracks in the ichnoassemblages where both the gracile and the robust morphotype have been identified, mainly levels BEB500, TCH1065 and CRO500. Level BEB500 (Fig. S1), the one with the highest number of studied tracks (n = 39), is mainly composed of sauropods (n = 17 trackways) and minute to small tridactyl (n = 158 trackways) tracks. No tracks assigned to *Jurabrontes curtedulensis* or *M. transjuranicus* have been documented in this level although it is the surface with the most Morphotype II tracks (n = 8 trackways) documented. Level TCH1065 (Fig. S2) (n = 15 studied tracks) is composed of 189 tracks, mainly of minute to small-sized theropods, and two parallel trackways (TCH1065-T26, TCH1065-T27) assigned to *Jurabrontes* have also been documented. In level CRO500 (Fig. S3) (n = 20 studied tracks), 16 sauropod trackways and 57 tridactyl trackways have been documented. One of the tridactyl trackways (CRO500-T43) has been assigned to Morphotype II (Razzolini et al., 2017). Thus, there are in three cases a large track type (Morphotype II in BEB500 and CRO500, and *Jurabrontes* in TCH1065) and the robust and the gracile morphotypes in the same surface (Figs. S1-S3). Interestingly, no *Megalosauripus* tracks have been documented in any of the three levels. One way to confirm that some of the small tracks were juveniles of the larger ichnospecies would be to find some kind of relationship among them, such as gregarious behaviour (*sensu* Castanera et al., 2014). However, there is no clear relationship between the trackways, neither of the same size nor of different sizes. In BEB500 (Fig. S1), trackways TR1, TR3, TR4, TR5, TR6 and TR8 (Morphotype II) cross several trackways made by small trackmakers, but the orientations are completely different and do not show any kind of relationship. TR2 (Morphotype II) is subparallel with T34 (small track but unknown morphotype) at the beginning of the trackway but shows a significant change in direction, so this does not show any relationship either. Notably, TR7 (Morphotype II) is a long trackway that is subparallel to T120 (robust morphotype). Tracks T120-L10 and T120-R10 tread over tracks TR7-R8 and TR7-L9 but pass afterwards, so although this might indicate some kind of interaction there is no clear evidence of gregarious behaviour. In level TCH1065 (Fig. S2), the two parallel trackways (TCH1065-T26, TCH1065-T27) assigned to *Jurabrontes* do not show any evidence of a relationship with the smaller tracks either. Finally,

in CRO500 (Fig. S3), T43 (Morphotype II) is slightly subparallel to T42 (small track but unknown morphotype), but there is no clear evidence to suggest that they were walking together. To sum up, generally the orientation of the large trackways does not seem to suggest any sort of relationship, with the possible exception of TR7 and T120. This single case might hint at the hypothesis that some tracks of the robust morphotype (BEB500-T120) might represent a juvenile of the producer of the tracks classified as Morphotype II. However, BEB500-T120 is the very trackway that shows more morphometric similarities to *Jurabrontes* than to Morphotype II (Fig. 6), thus weakening this hypothesis. In the light of the previous discussion, there is no evidence to suggest an interaction (i.e. behavioural aspect) among the dinosaurs that produced trackways of different sizes when they are left on the same surface. Thus, there is no indication (nor in footprint shape, nor morphometric, nor spatio-temporal) to suggest that the gracile and the robust morphotype are smaller tracks of the same of the larger morphotypes described from the area. Thus, the differences between the larger and the smaller morphotypes have thus led us to treat them as different ichnotaxa (see next section).

3) Ichnotaxonomy:

As noted by Marty (2008), small to medium-sized tridactyl tracks are generally not very common in the Late Jurassic and Early Cretaceous, and accordingly such tracks have only recently been the focus of ichnotaxonomic descriptions. Although recent descriptions have considerably increased the number of small to medium-sized tridactyl tracks, few ichnotaxa have been described in the Late Jurassic and Early Cretaceous of Europe. Lockley, Meyer and Moratalla (2000) suggested that theropod track morphologies are much more variable through time than previously thought. These authors pointed out that "the perception of morphological conservatism and uniformity through time is, in part, a function of lack of study of adequately large samples of well-preserved material (Baird, 1957)". In this sense, the studied tracks from the Ajoie ichnocoenosis represent a good sample of tridactyl dinosaur tracks in terms of the number of specimens (n = 93), with a considerable quality of preservation in many of them (n = 23 with a preservation grade greater than 2).

Although they are not very abundant in other European tracksites, small to medium-sized tridactyl trackways are the most abundant in the Ajoie ichnocoenosis. As mentioned above, the main small to medium-sized tridactyl dinosaur ichnotaxa that have been described from the Late Jurassic of Europe are (Fig. 7) *Grallator* (Fig. 7A) and *Anomoepus* (Fig. 7B) in Spain (Lockley et al., 2008; Piñuela, 2015; Castanera, Piñuela & García-Ramos, 2016); *Carmelopodus* (Fig. 7C) and *Eubrontes* (Fig. 7D) in France (Mazin et al., 2000; Mazin, Hantzpergue & Pouech, 2016); *Wildeichnus* isp. (Fig. 7E), cf. *Jialingpus* (Fig. 7F) and *Dineichnus* (Fig. 7G) in Poland (Gierliński, Niedźwiedzki & Nowacki, 2009); *Dineichnus* (Fig. 7H) (Lockley et al., 1998a) and *Therangospodus*-like tracks (Fig. 7I) (Lockley, Meyer & Moratalla, 2000) in Portugal; and *Grallator* in Germany (Fig. 7J) (Diedrich, 2011). In addition, Conti et al. (2005) described medium-sized footprints (Fig. 7K) that "resemble *Therangospodus*" (their type 3) and another

morphotype (their type 2, based on three specimens, Fig. 7L) that shares the same functional character with *Carmelopodus*, i.e., the lack of the fourth proximal pad on digit IV.

When compared with the type specimens of these ichnotaxa, the new data on the gracile morphotype of CRO500-T10 (Figs. 5A; 8N) (see previous sections) allow us to rule out the presence of *Carmelopodus untermannorum* (Fig. 8A) in the Ajoie, as previously discussed. Generally, the gracile morphotype (Fig. 8M-8O) does not fit with key features of the diagnosis of this ichnotaxon (Lockley et al., 1998b), differing in the phalangeal pad formula (2-3-4 rather than 2-3-3), symmetry, different length/width ratio, or the lower divarication. Among other theropod ichnotaxa, the gracile morphotype shows considerable differences with respect to *Wildeichnus navesi* (Fig. 8B, Casamiquela, 1964; Valais, 2011) from the Jurassic of Argentina (as well as larger size, a not subequal but lower divarication angle, larger claw marks, an unrounded digital phalangeal pad in digit IV, greater asymmetry, a generally higher length/width ratio); and with respect to *Therangospodus pandemicus* from the Late Jurassic of North America and Asia (Fig. 8C, smaller size, presence of clear phalangeal pads, higher mesaxony) (Lockley, Meyer & Moratalla, 2000; Fanti et al., 2013). The differences with respect to ornithopod ichnotaxa are noteworthy: it differs from *Anomoepus scambus* (Fig. 8D) in being less symmetric, having a metatarsal-phalangeal pad of digit IV not in line with the digit III axis, no hallux marks, higher mesaxony, and no manus prints present (see Olsen & Rainforth, 2003; Piñuela, 2015). It also differs notably with respect to *Dineichnus socialis* (Fig. 8E) for higher FL/FW ratio, higher mesaxony, no quadripartite morphology, a different heel pad impression, lower digit divarication (see Lockley et al., 1998a).

The features of the gracile morphotype fit better with the smaller ichnotaxa of the *Grallator-Anchisauripus-Eubrontes* (Fig. 8F-8H) plexus (Olsen, 1980; Demathieu, 1990; Weems, 1992; Olsen, Smith & McDonald, 1998): small to medium-sized, well-defined digital pads, digits II and IV of similar length, digit III being longer and showing high mesaxony, an oval/subrounded "heel" and a low interdigital angle. Although these footprints have mainly been described from Late Triassic and Early-Middle Jurassic deposits, in recent years they are also known from younger strata including the Late Jurassic of Europe (see Castanera, Piñuela & García-Ramos, 2016 and references therein). Regarding the use of the ichnotaxon *Anchisauripus*, Castanera, Piñuela & García-Ramos (2016) wrote a short review examining how different authors have considered *Grallator* and *Anchisauripus* as synonyms (Lucas et al., 2006; Lockley, 2009; Piñuela, 2015). The main sample of "grallatorid" tracks that has been described from Late Jurassic deposits in Europe comes from Asturias (Spain), and these have been assigned to *Grallator* (Castanera, Piñuela & García-Ramos, 2016). However, the gracile tracks from the Ajoie ichnocoenosis differ in the digit proportions (FL/FW ratio) and mesaxony (Fig. 9) from those in Asturias. It should be noted that the Asturian sample shows a great variation in mesaxony (that does not correlate with size). This holds also true for the gracile morphotype although the footprint proportions are less variable. Whereas Castanera, Piñuela & García-Ramos (2016) stated that mesaxony "should be used with caution in distinguishing between

different ichnotaxa", we consider that the differences in mesaxony between the gracile morphotype (AT =0.53-0.98) and the *Grallator* tracks from Asturias (AT =0.72-1.12, Castanera, Piñuela & García-Ramos 2016) tracks are large enough to do so. Furthermore, the FL/FW ratio is also considerably higher in the *Grallator* tracks (FL/FW ratio = 1.73-2.5, Castanera, Piñuela & García-Ramos 2016) than in the gracile morphotype (FL/FW ratio = 1.50-1.90). Oversplitting has occurred in some theropod ichnotaxa similar to *Grallator-Eubrontes* plexus. For example, Lockley et al. (2013) proposed a great reduction in the Jurassic theropod ichnotaxa from Asia, arguing that many of them were subjective junior synonyms of *Grallator* and *Eubrontes*. Nonetheless, the authors retain the ichnotaxon *Jialingpus yuechiensis* (Fig. 8I) from the Late Jurassic-Early Cretaceous of China (Xing et al., 2014). On the basis of digit proportions (FL/FW ratio) and mesaxony, the gracile morphotype falls partially within the range of *Jialingpus* but also within the range of *Kalohipus bretunensis* (Fig. 8J) from the Early Cretaceous (Berriasian) of Spain (Fuentes Vidarte & Meijide Calvo, 1998; Castanera et al., 2015). According to Xing et al. (2014), the main differences between *Jialingpus* and *Grallator* are the presence of a digit I trace and the large metatarsophalangeal area positioned in line with digit III, which are its main features. These features are absent in the gracile morphotype, so an assignment to *Jialingpus* can be excluded. On the other hand, the diagnosis of *Kalohipus bretunensis* (Fuentes Vidarte & Meijide Calvo, 1998) clearly includes features that distinguish it from the gracile morphotype, such as its smaller size or robust digits, and as seen in Fig. 9, the footprint proportions and especially the mesaxony are also slightly different. As mentioned above, the morphology is also different from the larger ichnotaxa (*Jurabrontes curtedulensis*, Fig. 8K, and *Megalosauripus transjuranicus*, Fig. 8L) that occur in the same deposits.

To summarize, the gracile morphotype is quite similar to other grallatorid tracks (*Grallator*, *Anchisauripus, Kalohipus, Jialingpus*), the main differences being the digit proportions and mesaxony. Given the current state of knowledge, it is difficult to interpret how much variation between the aforementioned ichnotaxa is a consequence of variations in preservation, ontogeny or ichnodiversity. Taking into account the whole discussion, and bearing in mind the high variation in both the FL/FW ratio and mesaxony seen in tracks assigned to *Grallator,* we thus tentatively classify the gracile morphotype as cf. *Kalohipus* isp., as this is the ichnotaxon that is closest to it (Fig. 9). Future studies should elucidate the similarities and differences between these grallatorid tracks. *Jialingpus* tracks have been also described in the Late Jurassic/Early Cretaceous of Europe (Gierliński, Niedźwiedzki & Nowacki, 2009), and an analysis of the differences between *Jialingpus* and other grallatorid tracks (including *Kalohipus*) is "pending" (Xing et al., 2014). In this regard, it would be interesting to note the differences in mesaxony among both *Kalohipus* and *Jialingpus* (low mesaxony) and *Grallator* (high mesaxony), and questioning whether mesaxony is a good measure for discriminating between the three ichnotaxa. Possible substrate related differences in preservation or ichnofacies substrates have to be tested too. For example, *Kalohipus bretunensis* and the main grallatorid ichnotaxa (Fig. 8F-J) are preserved in siliciclastic sediments whereas the tracks cf. *Kalohipus* isp. from the Swiss Jura Mountains are preserved in marginal marine carbonates.

Regarding the robust morphotype (Fig. 8P-8Q), a crucial question is whether it represents a single ichnotaxon. In this context, it should be noted that, the morphology of the tracks with a preservation grade of 2 or more, as well as the footprint proportions (Fig. 6B) such as those of trackway BEB500-T120 and the tracks from TCH1065 (TCH1065-T21-R1, TCH1065-E124 and TCH1065-E188) varies considerably. The appearance of this morphotype is completely different from ichnotaxa like *Carmelopodus untermannorum* (Fig. 8A, size, phalangeal pad formula, digit divarication, well-developed claw marks), *Wildeichnus navesi* (Fig. 8B, size, gracility, symmetry, length/width ratio and mesaxony), *Anomoepus scambus* (Fig. 8D, size, absence of a manus impression, morphology of the metatarsal-phalangeal pad of digit IV) and *Dineichnus socialis* (Fig. 8E, no quadripartite morphology or circular heel pad impression). It differs also from all the aforementioned grallatorid ichnotaxa *Grallator-Anchisauripus-Eubrontes*, plus *Jialingpus*, *Kalohipus* (Fig. 8F-J, mainly in the more robust morphology, footprint proportions, mesaxony, heel morphology, divarication) and the larger ichnotaxa (*Jurabrontes curtedulensis*, Fig. 8K, and *Megalosauripus transjuranicus*, Fig. 8L) that occur at the same localities..

Of all the known ichnotaxa, it shares most similarities with *Therangopodus pandemicus* (Fig. 8C, Lockley, Meyer & Moratalla, 2000; Fanti et al., 2013; see also Castanera et al., 2013 for new data on tracks previously assigned to *Therangospodus*), although the robust morphotype from the Swiss Jura Mountains has a higher digit divarication and probably higher mesaxony (unpublished data for this parameter in the original publication, Lockley, Meyer & Moratalla, 2000). According to the original diagnosis, this ichnotaxon is a "medium sized, elongate, asymmetric theropod track with coalesced, elongate, oval digital pads, not separated into discrete phalangeal pads". Trackway narrow with little or no rotation of digit III long axis from trackway axis". The tracks from the Ajoie ichnoassemblages are slightly smaller in size than *Therangospodus pandemicus* (Lockley, Meyer & Moratalla, 2000; Fanti et al., 2013). According to these authors, and based on the original descriptions by Lockley, Meyer & Moratalla (2000), *Therangospodus* is characterized by: "1) oval digital pads not separated into discrete digital pads, 2) no rotation of digit III, 3) narrow trackway, and 4) relatively reduced size (<30 cm in average length)". Regarding the absence of discrete digital pads, Lockley, Meyer & Moratalla (2000) described in the type ichnospecies of *Therangospodus* the presence of "faint indentations at the margin of the pads" that sometimes reveal the location of the phalangeal pads, suggesting a 2-3-4 phalangeal pad formula. Razzolini et al. (2017) also pointed out the difficulties of distinguishing between *Therangospodus* and *Megalosauripus*. This has also been previously discussed by other authors (Gierliński, Niedźwiedzki & Pieńkowski, 2001; Piñuela, 2015), suggesting that some of the diagnostic features might be extramorphological variations. It is notable that *Megalosauripus* and *Therangospodus* generally co-occur in the same sites (Meyer & Lockley, 1997; Lockley, Meyer & Moratalla, 2000; Lockley, Meyer & Santos, 2000; Xing, Harris & Gierliński, 2011; Fanti et al., 2013), which might be relevant as the size and preservation could be the only differences between the two ichnotaxa. Interestingly, as we have seen in the previous section, the robust morphotype does not co-occur with any *Megalosauripus* tracks, although some of them (BEB500-T120) co-occur with tracks described as Morphotype II. Even though the robust

643 morphotype is reminiscent of *Therangospodus pandemicus*, it is not possible to assign it to this
644 ichnospecies or to any of the known small-medium-sized ichnotaxa. The rarity of collected
645 specimens and the preservation grade (none of them as high as 2.5-3) prevents us from erecting a
646 new ichnotaxon. Taking into account that *Therangospodus pandemicus* is the closest ichnotaxon
647 described, we thus tentatively classify the tracks from level TCH1065 as cf. *Therangospodus* isp.
648 and the tracks from BEB500 as *Therangospodus*? isp. in order to show that there are some
649 differences (both morphometric and in shape) within the robust morphotype. As for the Swiss
650 specimens, *Therangospodus pandemicus* tracks have been preserved in carbonate materials
651 (Lockley, Meyer & Moratalla, 2000), so we can rule out the differences between this ichnotaxon
652 and the robust morphotype being a consequence of this factor as the substrate and the
653 palaeonvironmental conditions were probably similar at the time of track production.

654 CONCLUSIONS

655 The minute to medium-sized tridactyl dinosaur footprints from the tracksites of Highway A16 in
656 the Jura Mountains (NW Switzerland) represent one of the largest samples from the Late Jurassic
657 worldwide. The integrated analyses of the quality of preservation (preservation grade), the
658 maximum depth, the shape variation along the trackway, and the footprint proportions (FL/FW
659 ratio and mesaxony) open a new window into the interpretation of dinosaur track variations also
660 considering other factors such as preservation, ontogeny and ichnotaxonomy. The descriptions
661 and analyses of the material have made it possible to characterize in detail two different
662 morphotypes, one gracile and one robust, that were already identified in the field. The new data
663 allow us to rule out the notion that the two morphotypes represent a morphological continuum of
664 extramorphological variations, or ontogenetic variations of the larger tracks described from the
665 same sites. New morphometric data allow us to include the small sized tracks previously
666 described from Chevenez—Combe Ronde tracksite within the gracile morphotype, being the
667 only case in the studied sample that might be explained by an ontogenetic variation. An
668 ichnotaxonomical comparison with the main minute to medium-sized tridactyl ichnotaxa did not
669 allow assigning them to any known ichnotaxon with confidence. The gracile morphotype, though
670 similar to some grallatorid ichnotaxa, shows a number of morphometric differences and have
671 been assigned to cf. *Kalohipus* isp. The robust morphotype, though similar to *Therangospodus*
672 *pandemicus*, also shows some differences with respect to the diagnosis of the type specimen, and
673 therefore is classified as cf. *Therangospodus* isp. and *Therangospodus*? isp. Further work is
674 needed in order to understand the possible influence of the substrate composition on theropod
675 ichnotaxonomy in general and the aforementioned ichnotaxa in particular. This study also
676 highlights the difficulties of distinguishing between minute and medium-sized tridactyl dinosaur
677 ichnotaxa and the importance of analysing different factors related to preservation and ontogeny
678 before assigning a single track to a specific ichnotaxon. The new data increase theropod
679 ichnodiversity to 4/5? theropod ichnotaxa in the tidal flats of the Jura carbonate platform and
680 support previous suggestions that carbonate tidal flats were mainly dominated by theropod and
681 sauropod dinosaurs (Lockley,Hunt & Meyer 1994; D'Orazi Porchetti et al., 2016).

682

683 REFERENCES

684 Alcalá L, Mampel L, Royo-Torres R, Cobos A. 2014. On small quadrupedal ornithopod tracks in
685 Jurassic-Cretaceous transition intertidal deposits (El Castellar, Teruel, Spain). *Spanish Journal of*
686 *Palaeontology* 29 (2):83-190.

687 Antunes MT, Mateus O. 2003. Dinosaurs of Portugal. *Comptes Rendus Palevol* 2(1): 77-95.

688 Baird D. 1957. Triassic reptile footprint faunules from Milford, New Jersey. *Bulletin of The*
689 *Museum of Comparative Zoology* 117:449-520.

690 Belvedere M, Mietto P, Ishigaki S. 2010. A Late Jurassic diverse ichnocoenosis from the
691 siliciclastic Iouaridene Formation (Central High Atlas, Morocco). *Geological Quarterly*
692 54(3):367-380.

693 Belvedere M, Farlow JO. 2016. A numerical scale for quantifying the quality of preservation of
694 vertebrate tracks. In: Falkingham PL, Marty D, Richter A, eds. Dinosaur Tracks—The next
695 steps. Bloomington and Idianapolis: Indiana University Press. 92-99.

696 Bybee PJ, Lee AH, Lamm ET. 2006. Sizing the Jurassic theropod dinosaur *Allosaurus*: assessing
697 growth strategy and evolution of ontogenetic scaling of limbs. *Journal of Morphology* 267(3):
698 347-359.

699 Campos-Soto S, Cobos A, Caus E, Benito MI, Fernández-Labrador L, Suárez-Gonzalez P.,
700 Quijada E, Royo-Torres R, Mas R, Alcalá L. 2017. Jurassic Coastal Park: A great diversity of
701 palaeoenvironments for the dinosaurs of the Villar del Arzobispo Formation (Teruel, eastern
702 Spain). *Palaeogeography, Palaeoclimatology, Palaeoecology* 485: 154-177.

703 Casamiquela RM. 1964. Estudios icnológicos: problemas y métodos de la icnología con
704 aplicación al estudio de pisadas mesozoicas, Reptilia, Mammalia de la Patagonia. Librart.

705 Castanera D, Vila B, Razzolini NL, Falkingham PL, Canudo JI, Manning PL, Galobart À. 2013a.
706 Manus track preservation bias as a key factor for assessing trackmaker identity and
707 quadrupedalism in basal ornithopods. *PLOS ONE* 8(1), e54177.

708 Castanera D, Pascual C, Razzolini NL, Vila B, Barco JL, Canudo JI. 2013b.Discriminating
709 between medium-sized tridactyl trackmakers: tracking ornithopod tracks in the base of the
710 Cretaceous (Berriasian, Spain). *PLOS ONE* 8(11) e81830. doi: 10.1371/journal.pone.0081830.

711 Castanera D, Colmenar J, Sauqué V, Canudo JI. 2015. Geometric morphometric analysis applied
712 to theropod tracks from the Lower Cretaceous (Berriasian) of Spain. *Palaeontology* 58(1), 183-
713 200.

714 Castanera D, Piñuela L, García-Ramos JC. 2016. *Grallator* theropod tracks from the Late
715 Jurassic of Asturias (Spain): ichnotaxonomic implications. *Spanish Journal of Palaeontology*
716 31(2): 283-296.

717 Castanera D, Vila B, Razzolini NL, Santos VF, Pascual C, Canudo JI. 2014. Sauropod trackways
718 of the Iberian Peninsula: palaeoetological and palaeoenvironmental implications. *Journal of*
719 *Iberian Geology* 40(1): 49-59.

720 Clark ND, Ross DA, Booth P. 2005. Dinosaur tracks from the Kilmaluag Formation (Bathonian,
721 Middle Jurassic) of Score Bay, Isle of Skye, Scotland, UK. *Ichnos* 12(2): 93-104.

722 Comment G, Ayer J, Becker D. 2011. Deux nouveaux membres lithostratigraphiques de la
723 Formation de Reuchenette (Kimméridgien, Ajoie, Jura suisse)–Nouvelles données géologiques et
724 paléontologiques acquises dans le cadre de la construction de l'autoroute A16 (Transjurane).
725 *Swiss Bullettin for Applied Geology*16: 3-24.

726 Comment G, Lefort A, Koppka J, Hantzpergue P. 2015. Le Kimméridgien d'Ajoie (Jura, Suisse):
727 lithostratigraphie et biostratigraphie de la Formation de Reuchenette. *Revue de Paléobiologie* 34:
728 161-194.

729 Conti MA, Morsilli M, Nicosia U, Sacchi E, Savino V, Wagensommer A, Di Maggio L, Gianolla
730 P. 2005. Jurassic dinosaur footprints from southern Italy: footprints as indicators of constraints in
731 paleogeographic interpretation. *Palaios* 20(6): 534-550.

732 Demathieu GR. 1990. Problems in discrimination of tridactyl dinosaur footprints, exemplified by
733 the Hettangian trackways, the Causses, France. *Ichnos* 1(2): 97-110.

734 Diedrich C. 2011. Upper Jurassic tidal flat megatracksites of Germany –coastal dinosaur
735 migration highways between European islands, and a review of the dinosaur footprints.
736 *Palaeobiodiversity and Palaeoenvironments* 91: 129-155.

737 D´Orazi Porchetti S, Bernardi M, Cinquegranelli A, Santos VF, Marty D, Petti FM, Caetano PS,
738 Wagensommer, A. 2016. A Review of the Dinosaur Track Record from Jurassic and Cretaceous
739 Shallow Marine Carbonate Depositional Environments. In: Falkingham PL, Marty D, Richter A,
740 eds. Dinosaur Tracks—The next steps. Bloomington and Idianapolis: Indiana University Press.
741 380-392.

742 Falkingham PL. 2014. Interpreting ecology and behaviour from the vertebrate fossil track record.
743 *Journal of Zoology* 292(4): 222-228.

744 Fanti F, Contessi M, Nigarov A, Esenov P. 2013. New data on two large dinosaur tracksites from
745 the Upper Jurassic of Eastern Turkmenistan (Central Asia). *Ichnos* 20:54-71.

Farlow JO, Lockley MG. 1993. An Osteometric Approach to the Identification of the Makers of Early Mesozoic Tridactyl Dinosaur Footprints. In: Lucas SG, Morales M, eds. The nonmarine Triassic. *New Mexico Museum of Natural History and Science Bullletin*, 3: 123-131

Farlow JO, Holtz TRJ, Worthy TH, Chapman RE. 2013. Feet of the Fierce (and Not So Fierce): Pedal Proportions in Large Theropods, Other Non-Avian Dinosaurs, and Large Ground Birds. In: Parrish JM, Molnar RE, Currie PJ, Koppelhus EB, eds. Tyrannosaurid Paleobiology: Indiana University Press 89-132.

Foster JR, Lockley MG. 2006. The vertebrate ichnological record of the Morrison Formation (Upper Jurassic, north America). *New Mexico Museum of Natural History and Science Bullletin* 36: 203-216.

Fuentes Vidarte C, Meijide Calvo M. 1998. Icnitas de dinosaurios terópodos en el Weald de Soria (España). Nuevo icnogénero *Kalohipus*. *Estudios Geológicos* 54: 147-152.

Gatesy SM, Middleton KM, Jenkins Jr FA, Shubin NH. 1999. Three-dimensional preservation of foot movements in Triassic theropod dinosaurs. *Nature* 399(6732): 141-144.

Gierliński GD, Niedźwiedzki G, Pieńkowski G. 2001. Gigantic footprint of a theropod dinosaur in the Early Jurassic of Poland. *Acta Palaeontologica Polonica* 46(3): 441-446.

Gierliński GD, Niedźwiedzki G, Nowacki P. 2009. Small theropod and ornithopod footprints in the Late Jurassic of Poland. *Acta Geologica Polonica* 59(2): 221-234.

Griffin CT. 2018. Developmental patterns and variation among early theropods. *Journal of Anatomy*. doi: 10.1111/joa.12775

Gygi RA. 2000. Annotated index of lithostratigraphic units currently used in the Upper Jurassic of Northern Switzerland. *Eclogae Geologicae Helvetiae* 93: 125-146.

Hammer Ø, Harper DAT, Ryan PD. 2001. PAST: paleontological statistics software package for education and data analysis. *Palaeontologia Electronica* 4: 1-9.

Hornung JJ, Böhme A, Schlüter N, Reich M. 2016. In: Falkingham PL, Marty D, Richter A, eds. Dinosaur Tracks—The next steps. Bloomington and Idianapolis: Indiana University Press. 202-225.

Jank M, Wetzel A, Meyer CA. 2006. A calibrated composite section for the Late Jurassic Reuchenette Formation in northwestern Switzerland (?Oxfordian, Kimmeridgian *sensu gallico*, Ajoie-Region). *Eclogae Geologicae Helvetiae* 99: 175-191.

Kaever M, de Lapparent AF. 1974. Les traces de pas de dinosaures du Jurassique de Barkhausen (Basse Saxe, Allemagne). *Bulletin de la Société Géologique de France* 16: 516-525.

778 Lallensack JN, Sander PM, Knötschke N, Wings O. 2015. Dinosaur tracks from the Langenberg
779 Quarry (Late Jurassic, Germany) reconstructed with historical photogrammetry: evidence for
780 large theropods soon after insular dwarfism. *Palaeontologia Electronica* 18.2.31A: 1-34

781 Lallensack JN, van Heteren AH, Wings O. 2016. Geometric morphometric analysis of
782 intratrackway variability: a case study on theropod and ornithopod dinosaur trackways from
783 Münchehagen (Lower Cretaceous, Germany). *PeerJ* 4, e2059.

784 Lange-Badré B, Dutrieux M, Feyt J, Maury G. 1996. Découverte d'empreintes de pas de
785 dinosaures dans le Jurassique supérieur des Causses du Quercy (Lot, France).*Comptes rendus de*
786 *l'Académie des sciences*. Série 2. Sciences de la terre et des planets 323(1): 89-96.

787 Lockley MG. 1994. Dinosaur ontogeny and population structure: interpretations and speculations
788 based on fossil footprints. In: Carpenter K, Hirsch KF, Horner JR, eds. Dinosaur eggs and
789 babies. Cambridge University Press. 347-365.

790 Lockley MG. 2009. New perspectives on morphological variation in tridactyl footprints: clues to
791 widespread convergence in developmental dynamics. *Geological Quarterly* 53:415-432.

792 Lockley MG, Hunt AP, Meyer C. 1994. Vertebrate tracks and the ichnofacies concept:
793 implications for paleoecology and palichnostratigraphy. In: Donovan, SK, ed. The Palaeobiology
794 of Trace Fossils Wiley, 241-268.

795 Lockley MG, Santos VF, Meyer C, Hunt A. 1998a. A new dinosaur tracksite in the Morrison
796 Formation, Boundary Butte, Southeastern Utah. *Modern Geology* 23: 317-330.

797 Lockley M, Hunt A, Paquette M, Bilbey SA, Hamblin A.1998b. Dinosaur tracks from the
798 Carmel Formation, northeastern Utah: implications for Middle Jurassic paleoecology. *Ichnos*
799 5(4): 255-267.

800 Lockley MG, Meyer CA, Moratalla JJ. 2000. *Therangospodus*: trackway evidence for the
801 widespread distribution of a Late Jurassic theropod with well-padded feet. *Gaia* 15:339-353.

802 Lockley MG, Meyer CA, Santos VF. 2000. *Megalosauripus* and the problematic concept of
803 megalosaur footprints. *Gaia* 15:313-337.

804 Lockley M, Mitchell L, Odier GP. 2007. Small theropod track assemblages from Middle Jurassic
805 eolianites of Eastern Utah: paleoecological insights from dune ichnofacies in a transgressive
806 sequence. *Ichnos* 14(1-2): 131-142.

807 Lockley MG, Garcia-Ramos JC, Piñuela L, Avanzini M. 2008. A review of vertebrate track
808 assemblages from the Late Jurassic of Asturias, Spain with comparative notes on coeval
809 ichnofaunas from the western USA: implications for faunal diversity in siliciclastic facies
810 assemblages. *Oryctos* 8:53-70.

Lockley MG, Li JI, Li RH, Matsukawa M, Harris JD. Xing LD. 2013. A review of the tetrapod track record in China, with special reference to type ichnospecies: implications for ichnotaxonomy and paleobiology. *Acta Geologica Sinica* (English Edition) 87: 1-20.

Lucas SG, Klein H, Lockley MG, Spielmann JA, Gierliński GD, Hunt AP, Tanner LH. 2006. Triassic-Jurassic stratigraphic distribution of the theropod footprint ichnogenus *Eubrontes*. *New Mexico Museum of Natural History and Science Bulletin* 37: 86-93.

Mallison H, Wings O. 2014. Photogrammetry in paleontology—A practical guide. *Journal of Paleontological Techniques* 12: 1-31.

Marty D. 2008. Sedimentology, taphonomy, and ichnology of Late Jurassic dinosaur tracks from the Jura carbonate platform (Chevenez– Combe Ronde tracksite, NW Switzerland): insights into the tidalflat palaeoenvironment and dinosaur diversity, locomotion, and palaeoecology. *GeoFocus* 21:1-278.

Marty, D, Billon-Bruyat JP. 2009. Field-trip to the excavations in the Late Jurassic along the future Transjurane highway near Porrentruy (Canton Jura, NW Switzerland): dinosaur tracks, marine vertebrates and invertebrates. In: Billon-Bruyat JP, Marty D, Costeur L, Meyer CA, Thüring, B, eds. 5th International Symposium on Lithographic Limestone and Plattenkalk — Abstracts and Field Guides. Société jurassienne d'émulation, actes 2009 bis. p. 94-129

Marty D, Meyer CA. 2012. From sauropods to cycads – The Late Jurassic terrestrial record of the Swiss Jura Mountains. In: Witzmann F, Aberhan M, eds. Centen Meet Palaontologische Gesellschaft – Program Abstr F Guid Terra Nostra – Schriften der GeoUnion Alfred-Wegener-Stiftung, Potsadam. 119-120.

Marty D, Hug W, Iberg A, Cavin L, Meyer C, Lockley M. 2003. Preliminary Report on the Courtedoux Dinosaur Tracksite from the Kimmeridgian of Switzerland. *Ichnos* 10: 209-219.

Marty D, Cavin L, Hug WA, Jordan P, Lockley MG, Meyer CA. 2004.The protection, conservation and sustainable use of the Courtedoux dinosaur tracksite, Canton Jura, Switzerland. *Revue de Paléobiologie* 9:39-49.

Marty D, Ayer J, Becker D, Berger JP, Billon-Bruyat JP, Braillard L, Hug WA, Meyer CA. 2007. Late Jurassic dinosaur tracksites of the Transjurane highway (Canton Jura, NW Switzerland): overview and measures for their protection and valorisation. *Bulletin für Angewandte Geologie* 12: 75-89

Marty D, Strasser A, Meyer CA. 2009. Formation and taphonomy of human footprints in microbial mats of present-day tidal-flat environments: implications for the study of fossil footprints. *Ichnos* 16(1-2):127-142.

Marty D, Belvedere M, Meyer CA, Mietto P, Paratte G, Lovis C, Thüring B. 2010. Comparative analysis of Late Jurassic sauropod trackways from the Jura Mountains (NW Switzerland) and the central High Atlas Mountains (Morocco): implications for sauropod ichnotaxonomy. *Historical Biology* 22: 109-133.

Marty D, Meyer CA, Belvedere M, Ayer J, Schafer KL. 2013. Rochefort-Les Grattes: an early Tithonian dinosaur tracksite from the Canton Neuchatel, Switzerland. *Revue de Paléobiologie* 32: 373-384.

Marty D, Belvedere M, Razzolini NL, Paratte G, Cattin M, Lovis C, Meyer C. 2017. The tracks of giant theropods (*Jurabrontes curtedulensis* ichnogen. & ichnosp. nov.) from the Late Jurassic of NW Switzerland:palaeoecological and palaeogeographical implications. *Historical Biology* 1-29.

Matsukawa M, Lockley MG, Hunt AP.1999. Three age groups of ornithopods inferred from footprints in the mid-Cretaceous Dakota Group, eastern Colorado, North America.*Palaeogeography, Palaeoclimatology, Palaeoecology* 147(1): 39-51.

Matthews N, Noble T, Breithaupt B. 2016. Close-Range Photogrammetry for 3-D Ichnology: The Basics of Photogrammetric Ichnology. In: Falkingham PL, Marty D, Richter A, eds. Dinosaur Tracks—The next steps. Bloomington and Idianapolis: Indiana University Press. 28-55.

Mazin JM, Hantzpergue P, Bassoullet JP, Lafaurie G, Vignaud P.1997. The Crayssac site (Lower Tithonian, Quercy, Lot, France): discovery of dinosaur trackways in situ and first ichnological results. *Comptes Rendus de l'Academie des Sciences*. Series IIA Earth and Planetary Science 9(325): 733-739.

Mazin JM, Billon-Bruyat JP, Hantzpergue P, Lafaurie G. 2000. Domination reptilienne dans l'écosystème littoral de Crayssac (Tithonien inférieur, Quercy, Lot). *Bulletin de la Société herpétologique de France* 96: 71-81.

Mazin JM, Hantzpergue P, Pouech J. 2016. The dinosaur tracksite of Loulle (early Kimmeridgian; Jura, France). *Geobios* 49: 211-228.

Meyer CA. 1990. Sauropod tracks from the Upper Jurassic Reuchenette Formation (Kimmeridgian; Lommiswil, Kt. Solothurn) of Northern Switzerland. *Eclogae Geologicae Helvetiae* 83:389-397.

Meyer CA, Lockley MG.1997. Jurassic and Cretaceous dinosaur tracksites from Central Asia (Uzbekistan and Turkmenistan). In: Yang, SY, Huh M, Lee YN, Lockley MG, eds. *Paleontological Society of Korea, Special Publication* 2: 77-92.

Meyer CA, Thuring B. 2003. Dinosaurs of Switzerland. *Comptes Rendus –Palevol*. 2:103-117.

878 Milàn J, Bromley RG. 2006. True tracks, undertracks and eroded tracks, experimental work with
879 tetrapod tracks in laboratory and field. *Palaeogeography, Palaeoclimatology, Palaeoecology*
880 231(3): 253-264.

881 Moreau JD, Gand G, Fara E, Michelin A. 2012. Biometric and morphometric approaches on
882 Lower Hettangian dinosaur footprints from the Rodez Strait (Aveyron, France).*Comptes Rendus*
883 *Palevol* 11(4): 231-239.

884 Moreau JD, Néraudeau D, Vullo R, Abit D, Mennecart B, Schnyder J.2017. Late Jurassic
885 dinosaur footprints from Chassiron–La Morelière (Oléron Island, western France).
886 *Palaeobiodiversity and Palaeoenvironments* 97(4):773–789.

887 Olsen PE. 1980. Fossil Great Lakes of the Newark Supergroup in New Jersey. In: Manspeizer
888 W. ed. Field Studies of New Jersey Geology and Guide to Field Trips 52nd Annual Meeting
889 New York State Geology Association, Newark College of Arts and Sciences, Newark, Rutgers
890 University, 352-398.

891 Olsen PE, Rainforth EC. 2003. The Early Jurassic ornithischian dinosaurian ichnogenus
892 *Anomoepus*. In: LeTourneau PM, Olsen PE, eds. The Great Rift Valleys of Pangea in Eastern
893 North America, Volume 2: Sedimentology, Stratigraphy, and Paleontology, Columbia University
894 Press, 314-367.

895 Olsen PE, Smith JB, McDonald NG.1998. Type material of the type species of the classic
896 theropod footprint genera *Eubrontes*, *Anchisauripus*, and *Grallator* (Early Jurassic, Hartford and
897 Deerfield basins, Connecticut and Massachusetts, USA). *Journal of Vertebrate Paleontology* 18:
898 586-601.

899 Pascual-Arribas C, Hernández-Medrano N. 2011. Posibles huellas de crías de terópodo en el
900 yacimiento de Valdehijuelos (Soria, España). *Studia Geologica Salmanticensia* 47 (1): 77-110.

901 Piñuela L. 2015. *Huellas de dinosaurios y de otros reptiles del Jurásico Superior de Asturias*. D.
902 Phil. Thesis, Oviedo University.

903 Razzolini NL, Vila B, Castanera D, Falkingham PL, Barco JL, Canudo JI, Manning PL, Galobart
904 À. (2014). Intra-trackway morphological variations due to substrate consistency: The El Frontal
905 dinosaur tracksite (Lower Cretaceous, Spain). *PLOS ONE* 9(4), e93708.

906 Razzolini NL, Belvedere M, Marty D, Paratte G, Lovis C, Cattin M, Meyer CA. 2017.
907 *Megalosauripus transjuranicus* ichnosp. nov. A new Late Jurassic theropod ichnotaxon from
908 NW Switzerland and implications for tridactyl dinosaur ichnology and ichnotaxomy. *PLOS ONE*
909 12(7): e0180289

910 Santisteban C, Gaete R, Galobart A, Suñer M. 2003. Rastros de dinosaurios en el Jurásico
911 terminal (Facies Purbeck) de Corcolilla (Los Serranos, Valencia). In:Pérez Lorente F, Romero
912 Molina MM, Rivas Carrera, P, eds. Dinosaurios y otros reptiles mesozoicos en España. 33-40.

913 Santos VF. 2008. *Pegadas de dinossáurios de Portugal*. Museu Nacional de História Natural da
914 Universidade de Lisboa, Lisboa, 123 pp.

915 Schudack U, Schudack M, Marty D, Comment G. 2013. Kimmeridgian (Late Jurassic) ostracods
916 from Highway A16 (NW Switzerland): taxonomy, stratigraphy, palaeoecology, and
917 palaeobiogeography. *Swiss Journal of Geosciences* 106: 371-395.

918 Schulp AS, Al-Wosabi M. 2012. Telling apart ornithopod and theropod trackways: a closer look
919 at a large, Late Jurassic tridactyl dinosaur trackway at Serwah, Republic of Yemen. *Ichnos* 19(4):
920 194-198.

921 Stampfli G, Borel G. 2002. A plate tectonic model for the Paleozoic and Mesozoic constrained
922 by dynamic plate boundaries and restored synthetic oceanic isochrons. Earth and Planetary
923 Science Letters 196: 17-33.

924 Thierry J. 2000. Early Kimmeridgian. In: Dercourt J, Gaetani M, Vrielvynck B, Barrier E, Biju-
925 Duval B, Brunet MF, Cadet JP, Crasquin S, Sandulescu M, eds. Atlas Peri-Tethys,
926 Palaeogeographical maps—Explanatory Notes. CCGM/CGMN (Commission for the Geological
927 Map of the World), Paris: 85-97.

928 Thierry J, Barrier E, Abbate E, Alekseev AS, Ait-Salem H, Bouaziz S, et al. Map 10: Early
929 Kimmeridgian (146–144 Ma). 2000. In: Dercourt J, Gaetani M, Vrielvynck B, Barrier E, Biju-
930 Duval B, Brunet M, et al., editors. Atlas Peri-Tethys Palaeogeographical maps. CCGM/CGMN
931 (Commission for the Geological Map of the World), Paris.

932 Thulborn T. 1990. *Dinosaur tracks*. Chapman and Hall, London.

933 Valais SD.2011. Revision of dinosaur ichnotaxa from the La Matilde Formation (Middle
934 Jurassic), Santa Cruz Province, Argentina. *Ameghiniana* 48(1): 28-42.

935 .Waite R, Marty D, Strasser A, Wetzel A. 2013. The lost paleosols: Masked evidence for
936 emergence and soil formation on the Kimmeridgian Jura platform (NW Switzerland).
937 *Palaeogeography, Palaeoclimatology, Palaeoecology* 376: 73-90.

938 Weems RE. 1992. A re-evaluation of the taxonomy of Newark Supergroup saurischian dinosaur
939 tracks, using extensive statistical data from a recently exposed tracksite near Culpeper, Virginia.
940 In: Sweet PC, editor. Proceedings of the 26th forum on the geology of industrial minerals, 119:
941 113-127.

942 Wilson JA, Marsicano CA, Smith RM. 2009. Dynamic locomotor capabilities revealed by early
943 dinosaur trackmakers from Southern Africa. *PLoS One*, *4*(10), e7331.

Xing LD, Harris JD, Gierliński G. 2011. *Therangospodus* and *Megalosauripus* track assemblage from the Upper Jurassic–Lower Cretaceous Tuchengzi Formation of Chicheng County, Hebei Province, China and their paleoecological implications. *Vertebrata PalAsiatica* 49(4): 423-434.

Xing LD, Lockley MG, Klein H, Gierliński GD, Divay JD, Hu SM, Zhang JP, Ye Y, He YP. 2014. The non-avian theropod track *Jialingpus* from the Cretaceous of the Ordos Basin, China, with a revision of the type material: implications for ichnotaxonomy and trackmaker morphology. *Palaeoworld* 23:187-199.

Xing LD, Lockley MG, Hu N, Li G, Tong G, Matsukawa M, Klein H, Ye Y, Zhang J, Persons WS. 2016. Saurischian track assemblages from the Lower Cretaceous Shenhuangshan Formation in the Yuanma Basin, Southern China. *Cretaceous Research* 65: 1-9.

FIGURE CAPTIONS:

Fig. 1: Geographical and geological settings of the tracksites (modified from Razzolini et al., 2017; Marty et al., 2017). A) Geographical setting of the Ajoie district (NW Switzerland) with the location of the tracksites (1- Courtedoux—Béchat Bovais, 2- Courtedoux—Bois de Sylleux, 3- Courtedoux—Tchâfouè, 4- Courtedoux—Sur Combe Ronde, 5- Chevenez—Combe Ronde, 6- Chevenez—La Combe) along Highway A16. B) Chrono-, bio- and lithostratigraphic setting of the Reuchenette Formation in the Ajoie district, Canton Jura, NW Switzerland (after Comment, Ayer & Becker, 2011, 2015). Source credit: OCC-SAP, Canton Jura.

Fig. 2: Pictures and false-colour depth maps of the tracks with a high preservation grade that belong to the gracile morphotype. A) BEB500-T16-R3; B) BEB500-T26-R5; C) BEB500-T73-L5; D) BSY1020-E2; E) CHV1000-E4; F) CRO500-T10-L10; G) SCR1055-T2-L2*; H) SCR1055-T3-L2*; I) TCH1055-E53; J) TCH1055-T2-L1; K) TCH1060-E58; L) TCH1065-E3; M) TCH1065-E177; N) TCH1065-T25-L2; O) TCH1069-T1-R2. *In these two cases, it is not a picture but a coloured mesh obtained from the 3D-model. Scale bar = 5 cm. Source credit: OCC-SAP, Canton Jura.

Fig. 3: Pictures and false-colour depth maps of the tracks with a high preservation grade that belong to the robust morphotype. A) BEB500-T120-R5; B) BEB500-T120-R6; C) TCH1065-T21-R1; D) TCH1065-E188; E) TCH1065-E124; F) TCH1065-T15-R1. Scale bar = 5 cm. Source credit: OCC-SAP, Canton Jura.

Fig. 4: Morphological variation in the footprint shape along the studied trackways from BEB500 tracksite. A) BEB500-T16 (gracile morphotype); B) BEB500-T17 (gracile morphotype); C) BEB500-T58 (gracile morphotype); D) BEB500-T73 (gracile morphotype); E) BEB500-T75 (gracile morphotype); F) BEB500-T78 (gracile morphotype); G) BEB500-T82 (gracile

morphotype); H) BEB500-T120 (robust morphotype). I) BEB500-T93 (gracile morphotype). Source credit: OCC-SAP, Canton Jura.

Fig. 5: Morphological variation in the footprint shape along the studied trackways from the CRO500, TCH1055, TCH1065 and TCH1069 tracksites. A) CRO500-T10 (gracile morphotype); B) CRO500-T30BIS (gracile morphotype); C) TCH1055-T2 (gracile morphotype); D) TCH1065-T15 (robust morphotype); E) TCH1069-T2 (robust morphotype); F) TCH1065-T25 (gracile morphotype). Source credit: OCC-SAP, Canton Jura.

Fig. 6: Bivariate graph plotting the footprint length/footprint width ratio against the mesaxony (AT) of the studied tracks (gracile and robust morphotype) with the larger tracks described in the Reuchenette Formation. A) Gracile and robust morphotype compared with *Megalosauripus* tracks (including tracks classified as *Megalosauripus transjuranicus*, *Megalosauripus* cf. *transjuranicus* and *Megalosauripus* isp.), the Morphotype II tracks and *Jurabrontes curtedulensis* (after Razzolini et al., 2017; Marty et al., 2017). Note that in many cases the points represent tracks from the same trackway, so variation through the trackway is also represented. B) The studied tracks compared with just the holotype and paratype specimens of *Megalosauripus transjuranicus* and *Jurabrontes curtedulensis*, plus the best-preserved tracks of Morphotype II (BEB500-TR7). Outline drawings not to scale. The specimen in red is CRO500-T10-L10 (previously classified as *Carmelopodus* and herein consider as part of the gracile morphotype, see discussion). Source credit: OCC-SAP, Canton Jura.

Fig. 7: Main small-medium-sized tridactyl dinosaur footprints described in the Late Jurassic of Europe. A) *Grallator* from Spain (S, after Castanera, Piñuela & García-Ramos, 2016); B) *Anomoepus* from Spain (S, after Piñuela, 2015); C) *Carmelopodus* from France (C, after Mazin, Hantzpergue & Pouech, 2016); D) *Eubrontes* from France (C, after Mazin et al., 2000); E) *Wildeichnus* from Poland (C, after Gierliński, Niedźwiedzki & Nowacki, 2009); F) *Jialingpus* from Poland (C, after Gierliński, Niedźwiedzki & Nowacki, 2009). G) *Dineichnus* from Poland (C, after Gierliński, Niedźwiedzki & Nowacki, 2009); H) *Dineichnus* from Portugal (S, Lockley et al., 1998a); I) *Therangospodus*-like track from Portugal (S, after Lockley, Meyer & Moratalla, 2000; J) *Grallator* from Germany (S, after Diedrich, 2011). K) *Therangospodus*-like track from Italy (C, after Conti et al., 2005); L) *Carmelopodus*-like track from Italy (C, after Conti et al., 2005). Scale bar = 1cm (E), 5 cm (A, F, G), 10 cm (B, C, D, H, I, J, K, L). S and C refer to siliciclastic and carbonate substrate, respectively. Source credit: OCC-SAP, Canton Jura.

Fig. 8: A) Outline drawing of the holotype of *Carmelopodus untermannorum* (S, redrawn after Lockley et al., 1998b); B) Outline drawing of the holotype of *Wildeichnus navesi* (V, redrawn after Lockley, Mitchel & Odier, 2007); C) Outline drawing of the topotype of *Therangospodus pandemicus* (S, after Lockley, Meyer & Moratalla, 2000); D) Outline drawing of *Anomoepus scambus* (S, after Olsen & Rainforth, 2003); E) Outline drawing of the holotype of *Dineichnus socialis* (S, after Lockley et al., 1998a); F) Composite outline drawing of type trackway of *Grallator parallelus* (S, redrawn from Olsen, Smith & McDonald, 1998); G) Outline drawing of

type specimen of *Anchisauripus sillimani* (S, redrawn from Olsen, Smith & McDonald, 1998); H) Outline drawing of type specimen of *Eubrontes giganteus* (S, redrawn from Olsen, Smith & McDonald, 1998). I) Outline drawing of type specimen of *Jialingpus yuechiensis* (S, redrawn from Lockley et al., 2013); J) Outline drawing of type specimen of *Kalohipus bretunensis* (S, redrawn from Fuentes Vidarte & Meijide Calvo, 1998). K) Outline drawing of type specimen of *Jurabrontes curtedulensis* (redrawn from Marty et al., 2017). L) Outline drawing of type specimen of *Megalosauripus transjuranicus* (redrawn from Razzolini et al., 2017). M) Outline drawing of specimen BSY1020-E2 (cf. *Kalohipus* isp.). N) Outline drawing of specimen CRO500-T10-L10 (cf. *Kalohipus* isp.). O) Outline drawing of specimen TCH-1060-E58 (cf. *Kalohipus* isp.); P) Outline drawing of specimen TCH-1065-T21-R1 (cf. *Therangospodus* isp.). Q) Outline drawing of specimen BEB500-T120-R5 (*Therangospodus*? isp.). S, C and V refer to siliciclastic, carbonate and volcanoclastic substrate, respectively. Scale bar = 2 cm (B, D), 5 cm (F,G, H, I, J), 10 cm (A, C, E, L, M-Q), 50 cm (K). Source credit: OCC-SAP, Canton Jura.

Fig. 9: Bivariate graph plotting the footprint length/footprint width ratio *vs* AT of the studied tracks (gracile and robust morphotype) with some of the main dinosaur tridactyl ichnotaxa mentioned in the text. Outline drawings not to scale. Source credit: OCC-SAP, Canton Jura.

Table 1: Measurements of the specimens with a high preservation grade: footprint length (FL), footprint width (FW), footprint length /footprint width ratio (FL/FW), digit length (LI, LII, LIII), digit width (WI, WII, WIII), divarication angles (II-III, III-IV), mesaxony (AT, anterior triangle ratio; ATw, anterior triangle width; ATl, anterior triangle length).

Table 2: Variation in preservation grade and variation in maximum depth (difference between highest and lowest value) through the analysed trackways (see Table S1 for specific values of each track).

Supplemental information Table S1: List of the specimens analysed, their quality of preservation (preservation grade) and the maximum depth. Those with preservation grade 0-0.5 are not included in the figshare file. The tracks where the variation along the trackway has been analysed are in red.

Supplemental information Figure S1: Map of the Courtedoux—Béchat Bovais tracksite, level 500 (BEB500). In red (gracile) and blue (robust) the minute to medium-sized tridactyl tracks and in green, the larger morphtoype (Morphotype II). Source credit: OCC-SAP, Canton Jura.

Supplemental information Figure S2: Map of the Courtedoux—Tchâfouè tracksite, level 1065 (TCH1065). In red (gracile) and blue (robust) the minute to medium-sized tridactyl tracks and in green, the larger morphtoype (*Jurabrontes curtedulensis* see Marty et al., 2017). Source credit: OCC-SAP, Canton Jura.

Supplemental information Figure S3: Map of the Chevenez—Combe Ronde, level 500 (CRO500). In red (gracile) and blue (robust) the minute to medium-sized tridactyl tracks and in green, the larger morphtoype (Morphotype II). Source credit: OCC-SAP, Canton Jura.

Acknowledgements

We thank all technicians, photographers, geometers, drawers, collection managers, and preparators of the PALA16 that were involved during the excavation and documentation of the tracksites and during the set-up and organization of the track collection. We also thank the scientific staff of the PALA16 and JURASSICA Muséum for various stimulating discussions and valuable input. The authors also thank Laura Piñuela, Vanda Santos, Ignacio Díaz-Martínez, Oliver W.M. Rauhut and Novella L. Razzolini for fruitful discussion on the topic of this manuscript. The comments of the editor (Claudia Marsicano) and the reviewers (Jesper Milàn and Verónica Krapovickas) have considerably improved the quality of the manuscript and are greatly appreciated. Rupert Glasgow revised the English grammar.

Figure 1

Geographical and geological settings of the Highway 16 tracksites (modified from Razzolini et al., 2017; Marty et al., 2017).

A) Geographical setting of the Ajoie district (NW Switzerland) with the location of the tracksites (1- Courtedoux—Béchat Bovais, 2- Courtedoux—Bois de Sylleux, 3- Courtedoux—Tchâfouè, 4- Courtedoux—Sur Combe Ronde, 5- Chevenez—Combe Ronde, 6- Chevenez—La Combe) along Highway A16. B) Chrono-, bio- and lithostratigraphic setting of the Reuchenette Formation in the Ajoie district, Canton Jura, NW Switzerland (after Comment, Ayer & Becker, 2011, 2015). Source credit: OCC-SAP, Canton Jura.

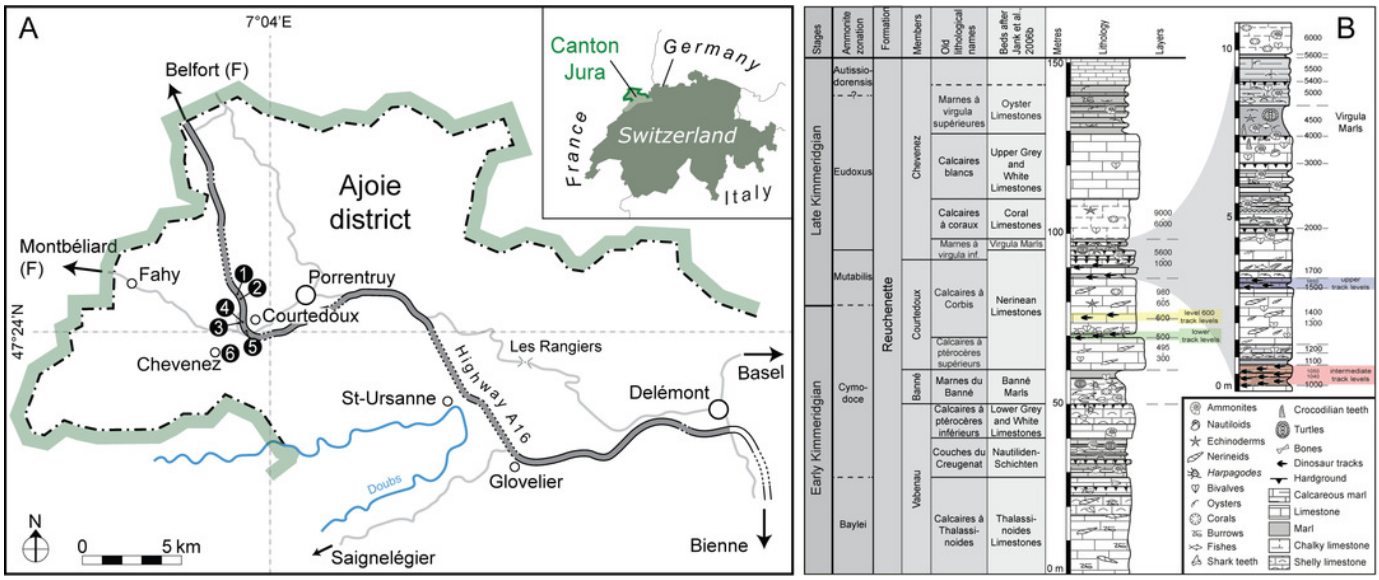

Figure 2

Pictures and false-colour depth maps of the tracks with a high preservation grade that belong to the gracile morphotype.

A) BEB500-T16-R3; B) BEB500-T26-R5; C) BEB500-T73-L5; D) BSY1020-E2; E) CHV1000-E4; F) CRO500-T10-L10; G) SCR1055-T2-L2*; H) SCR1055-T3-L2*; I) TCH1055-E53; J) TCH1055-T2-L1; K) TCH1060-E58; L) TCH1065-E3; M) TCH1065-E177; N) TCH1065-T25-L2; O) TCH1069-T1-R2. *In these two cases, it is not a picture but a coloured mesh obtained from the 3D-model. Scale bar = 5 cm. Source credit: OCC-SAP, Canton Jura.

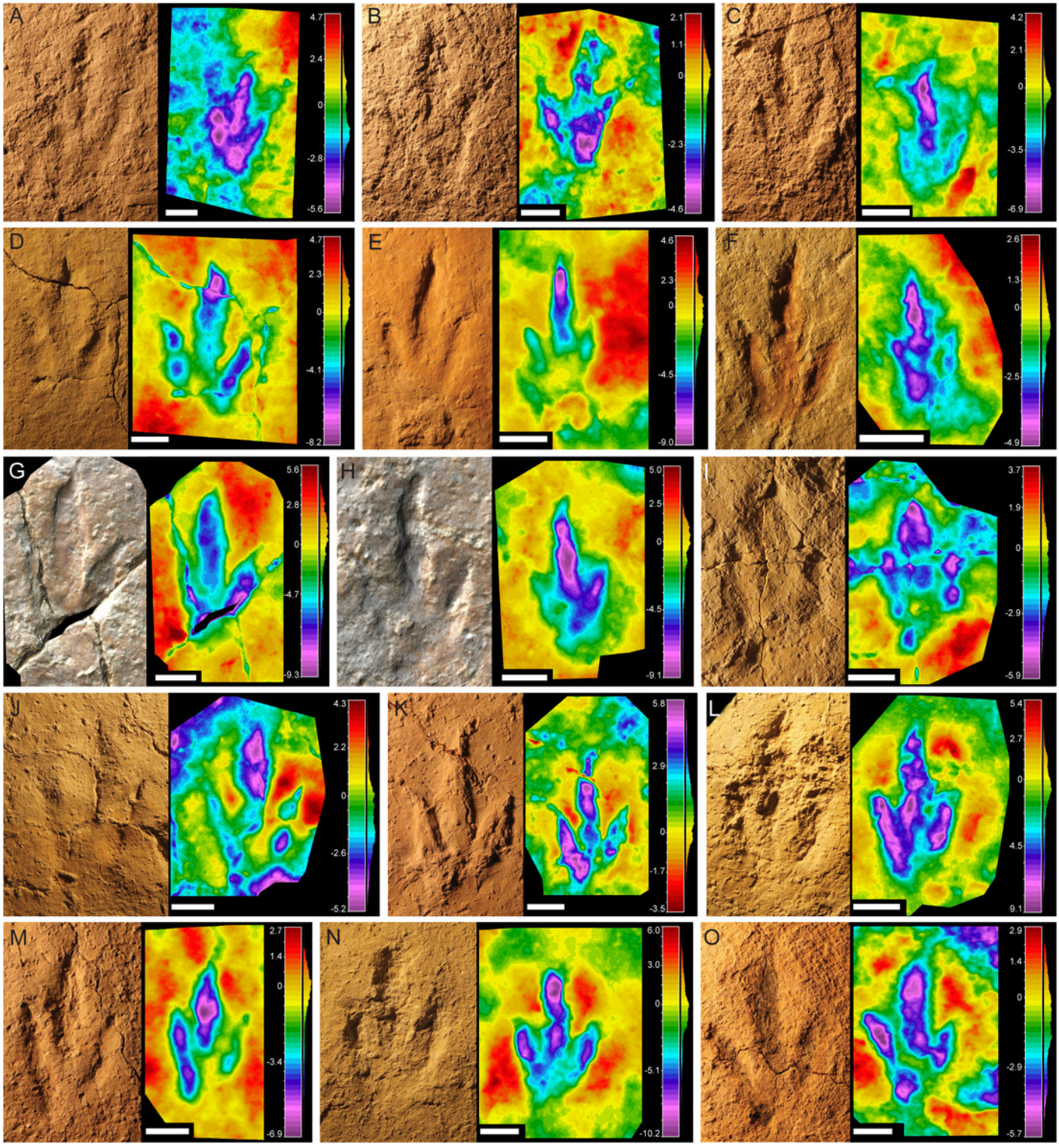
A
4.7
2.4
0
-2.8
-5.6
B
2.1
1.1
0
-2.3
-4.6
C
4.2
2.1
0
-3.5
-6.9
D
4.7
2.3
0
-4.1
-8.2
E
4.6
2.3
0
-4.5
-9.0
F
2.6
1.3
0
-2.5
-4.9
G
5.6
2.8
0
-4.7
-9.3
H
5.0
2.5
0
-4.5
-9.1
I
3.7
1.9
0
-2.9
-5.9
J
4.3
2.2
0
-2.6
-5.2
K
5.8
2.9
0
-1.7
-3.5
L
5.4
2.7
0
4.5
9.1
M
2.7
1.4
0
-3.4
-6.9
N
6.0
3.0
0
-5.1
-10.2
O
2.9
1.4
0
-2.9
-5.7

Figure 3

Pictures and false-colour depth maps of the tracks with a high preservation grade that belong to the robust morphotype.

A) BEB500-T120-R5; B) BEB500-T120-R6; C) TCH1065-T21-R1; D) TCH1065-E188; E) TCH1065-E124; F) TCH1065-T15-R1. Scale bar = 5 cm. Source credit: OCC-SAP, Canton Jura.

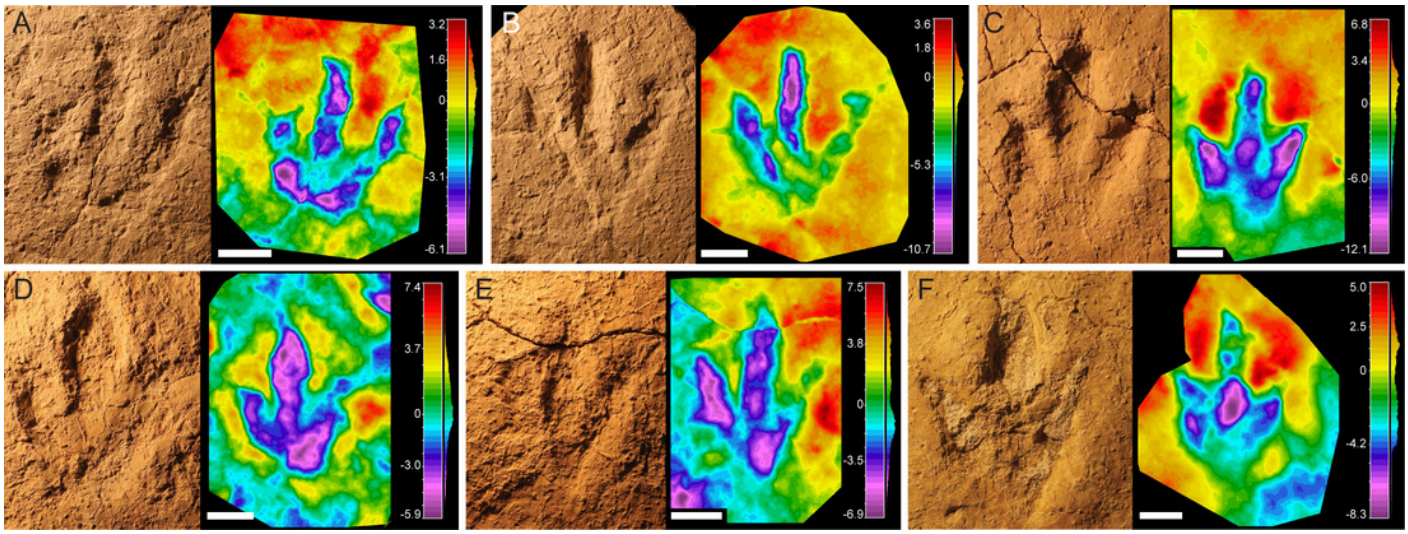

Figure 4

Morphological variation in the footprint shape along the studied trackways from BEB500 tracksite.

A) BEB500-T16 (gracile morphotype); B) BEB500-T17 (gracile morphotype); C) BEB500-T58 (gracile morphotype); D) BEB500-T73 (gracile morphotype); E) BEB500-T75 (gracile morphotype); F) BEB500-T78 (gracile morphotype); G) BEB500-T82 (gracile morphotype); H) BEB500-T120 (robust morphotype). I) BEB500-T93 (gracile morphotype). Source credit: OCC-SAP, Canton Jura.

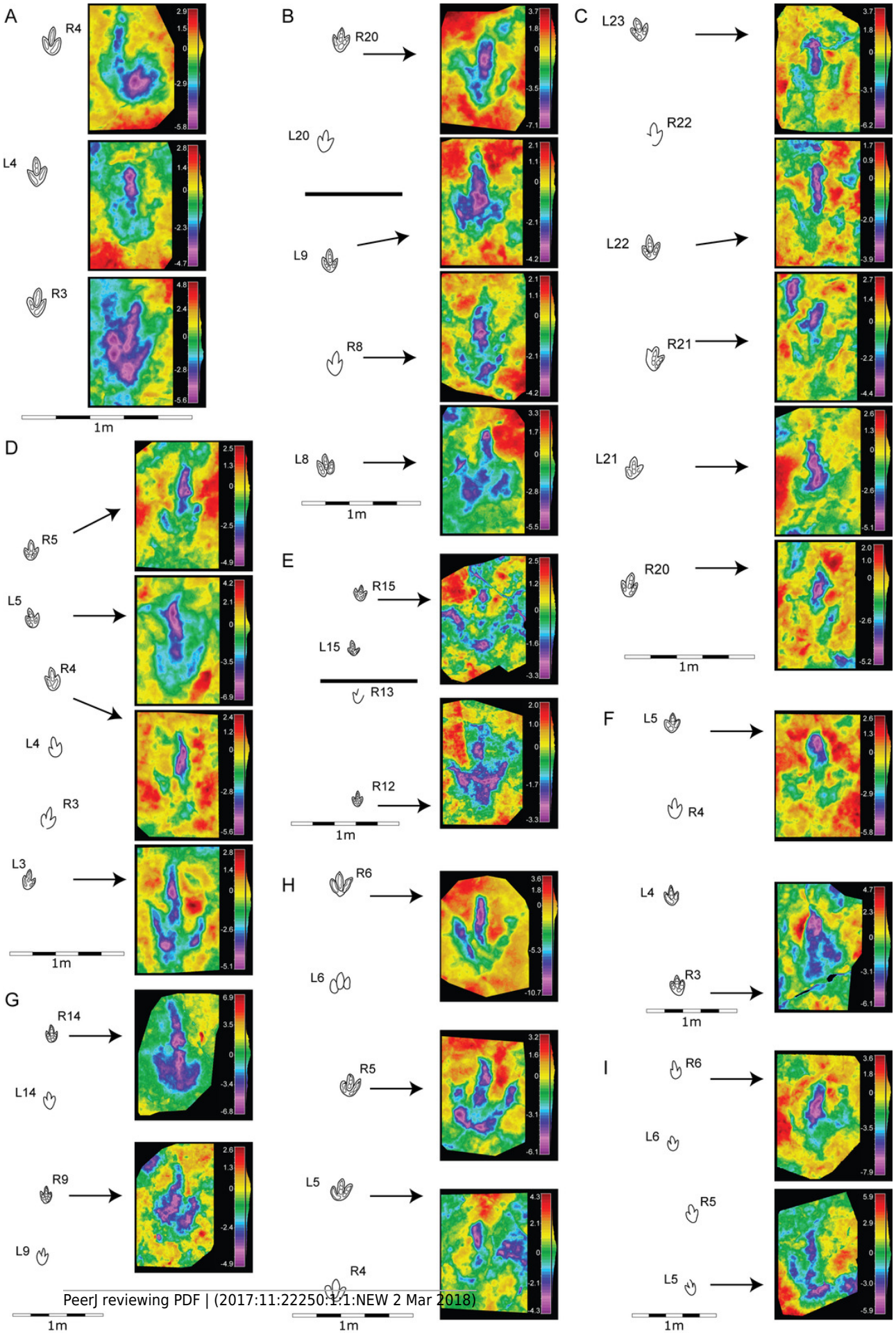
A
R4
L4
R3
1m
B
R20
L20
L9
R8
L8
1m
C
L23
R22
L22
R21
L21
R20
1m
D
R5
L5
R4
L4
R3
L3
1m
E
R15
L15
R13
R12
1m
F
L5
R4
L4
R3
1m
G
R14
L14
R9
L9
1m
H
R6
L6
R5
L5
R4
1m
I
R6
L6
R5
L5
1m

Figure 5

Morphological variation in the footprint shape along the studied trackways from the CRO500, TCH1055, TCH1065 and TCH1069 tracksites.

A) CRO500-T10 (gracile morphotype); B) CRO500-T30BIS (gracile morphotype); C) TCH1055-T2 (gracile morphotype); D) TCH1065-T15 (robust morphotype); E) TCH1069-T2 (robust morphotype); F) TCH1065-T25 (gracile morphotype). Source credit: OCC-SAP, Canton Jura.

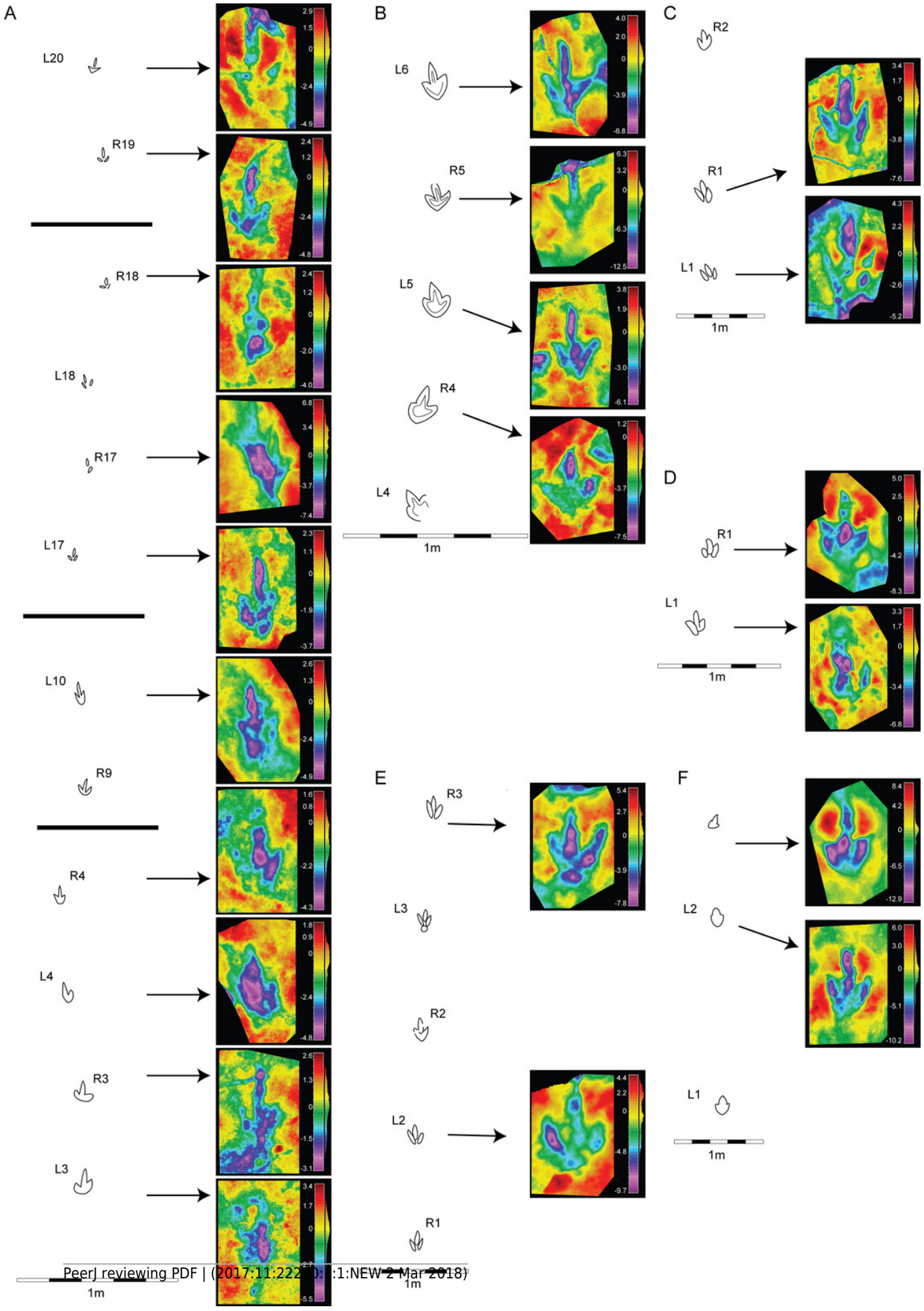
A
L20
R19
R18
L18
R17
L17
L10
R9
R4
L4
R3
L3
1m
B
L6
R5
L5
R4
L4
1m
C
R2
R1
L1
1m
D
R1
L1
1m
E
R3
L3
R2
L2
R1
1m
F
L2
L1
1m

Figure 6

Bivariate graph plotting the footprint length/footprint width ratio against the mesaxony (AT) of the studied tracks (gracile and robust morphotype) with the larger tracks described in the Reuchenette Formation.

A) Gracile and robust morphotype compared with *Megalosauripus* tracks (including tracks classified as *Megalosauripus transjuranicus*, *Megalosauripus* cf. *transjuranicus* and *Megalosauripus* isp.), the Morphotype II tracks and *Jurabrontes curtedulensis* (after Razzolini et al., 2017; Marty et al., 2017). Note that in many cases the points represent tracks from the same trackway, so variation through the trackway is also represented. B) The studied tracks compared with just the holotype and paratype specimens of *Megalosauripus transjuranicus* and *Jurabrontes curtedulensis*, plus the best-preserved tracks of Morphotype II (BEB500-TR7). Outline drawings not to scale. The specimen in red is CRO500-T10-L10 (previously classified as *Carmelopodus* and herein consider as part of the gracile morphotype, see discussion). Source credit: OCC-SAP, Canton Jura.

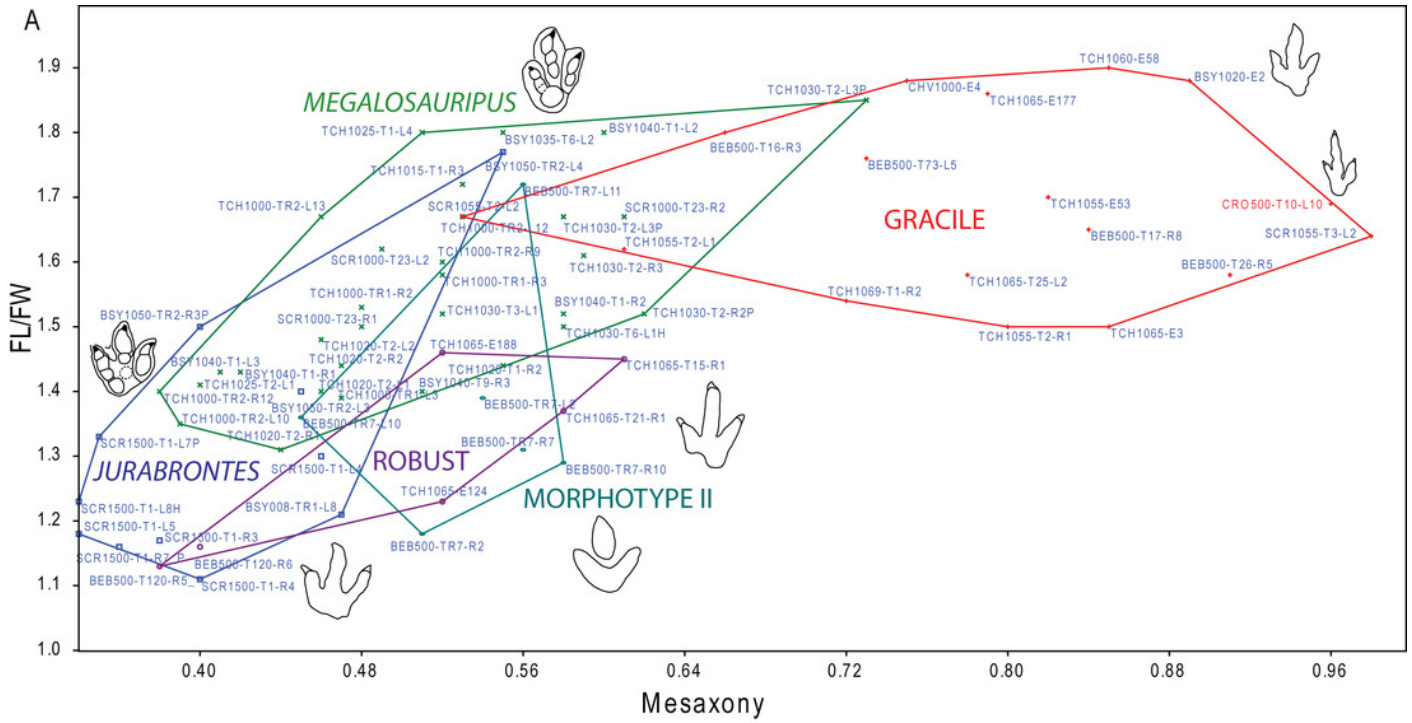
A
FL/FW
Mesaxony
MEGALOSAURIPUS
GRACILE
ROBUST
JURABRONTES
MORPHOTYPE II
TCH1060-E58
BSY1020-E2
CHV1000-E4
TCH1065-E177
TCH1030-T2-L3P
BEB500-T16-R3
BEB500-T73-L5
TCH1055-E53
CRO500-T10-L10
BEB500-T17-R8
SCR1055-T3-L2
BEB500-T26-R5
TCH1065-T25-L2
TCH1069-T1-R2
TCH1055-T2-R1
TCH1065-E3
TCH1025-T1-L4
BSY1035-T6-L2
BSY1040-T1-L2
TCH1015-T1-R3
BSY1050-TR2-L4
BEB500-TR7-L11
TCH1000-TR2-L13
SCR1055-T2-L2
SCR1000-T23-R2
TCH1000-TR2-12
TCH1030-T2-L3P
TCH1055-T2-L1
SCR1000-T23-L2
TCH1000-TR2-R9
TCH1030-T2-R3
TCH1000-TR1-R2
TCH1000-TR1-R3
BSY1050-TR2-R3P
SCR1000-T23-R1
TCH1030-T3-L1
BSY1040-T1-R2
TCH1030-T2-R2P
TCH1030-T6-L1H
TCH1020-T2-L2
TCH1065-E188
BSY1040-T1-L3
TCH1020-T2-R2
TCH1065-T15-R1
BSY1040-T1-R1
TCH1025-T2-L1
BSY1040-T9-R3
TCH1000-TR2-R12
BEB500-TR7-L2
BSY1050-TR2-L3
TCH1065-T21-R1
TCH1000-TR2-L10
BEB500-TR7-L10
SCR1500-T1-L7P
TCH1020-T2-R1
BEB500-TR7-R7
SCR1500-T1-L1
BEB500-TR7-R10
TCH1065-E124
SCR1500-T1-L8H
BSY008-TR1-L8
SCR1500-T1-L5
SCR1500-T1-R3
BEB500-TR7-R2
SCR1500-T1-R7_P
BEB500-T120-R6
BEB500-T120-R5
SCR1500-T1-R4

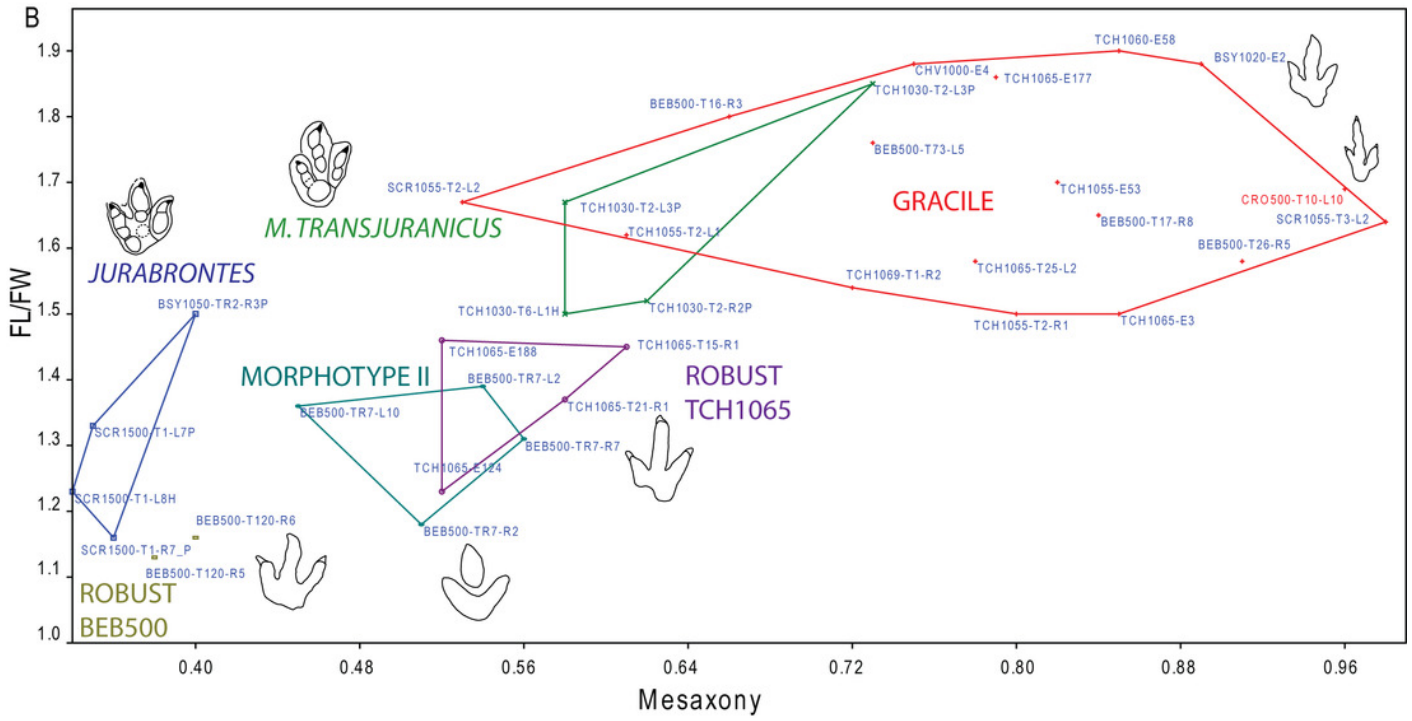
B
FL/FW
Mesaxony
M. TRANSJURANICUS
JURABRONTES
GRACILE
MORPHOTYPE II
ROBUST
TCH1065
ROBUST
BEB500
TCH1060-E58
BSY1020-E2
CHV1000-E4
TCH1065-E177
TCH1030-T2-L3P
BEB500-T16-R3
BEB500-T73-L5
SCR1055-T2-L2
TCH1055-E53
CRO500-T10-L10
BEB500-T17-R8
SCR1055-T3-L2
BEB500-T26-R5
TCH1065-T25-L2
TCH1069-T1-R2
TCH1055-T2-L1
TCH1055-T2-R1
TCH1065-E3
BSY1050-TR2-R3P
TCH1030-T6-L1H
TCH1030-T2-R2P
TCH1065-E188
TCH1065-T15-R1
BEB500-TR7-L2
BEB500-TR7-L10
TCH1065-T21-R1
SCR1500-T1-L7P
BEB500-TR7-R7
TCH1065-E124
SCR1500-T1-L8H
BEB500-TR7-R2
BEB500-T120-R6
SCR1500-T1-R7_P
BEB500-T120-R5

Figure 7

Main small-medium-sized tridactyl dinosaur footprints described in the Late Jurassic of Europe.

A) *Grallator* from Spain (S, after Castanera, Piñuela & García-Ramos, 2016); B) *Anomoepus* from Spain (S, after Piñuela, 2015); C) *Carmelopodus* from France (C, after Mazin, Hantzpergue & Pouech, 2016); D) *Eubrontes* from France (C, after Mazin et al., 2000); E) *Wildeichnus* from Poland (C, after Gierliński, Niedźwiedzki & Nowacki, 2009); F) *Jialingpus* from Poland (C, after Gierliński, Niedźwiedzki & Nowacki, 2009). G) *Dineichnus* from Poland (C, after Gierliński, Niedźwiedzki & Nowacki, 2009); H) *Dineichnus* from Portugal (S, Lockley et al., 1998a); I) *Therangospodus*-like track from Portugal (S, after Lockley, Meyer & Moratalla, 2000; J) *Therangospodus*-like track from Italy (C, after Conti et al., 2005). K) *Carmelopodus*-like track from Italy (C, after Conti et al., 2005); L) *Grallator* from Germany (S, after Diedrich, 2011). Scale bar = 1cm (E), 5 cm (A, F, G), 10 cm (B, C, D, H, I, J, K, L). S and C refer to siliciclastic and carbonate substrate, respectively. Source credit: OCC-SAP, Canton Jura.

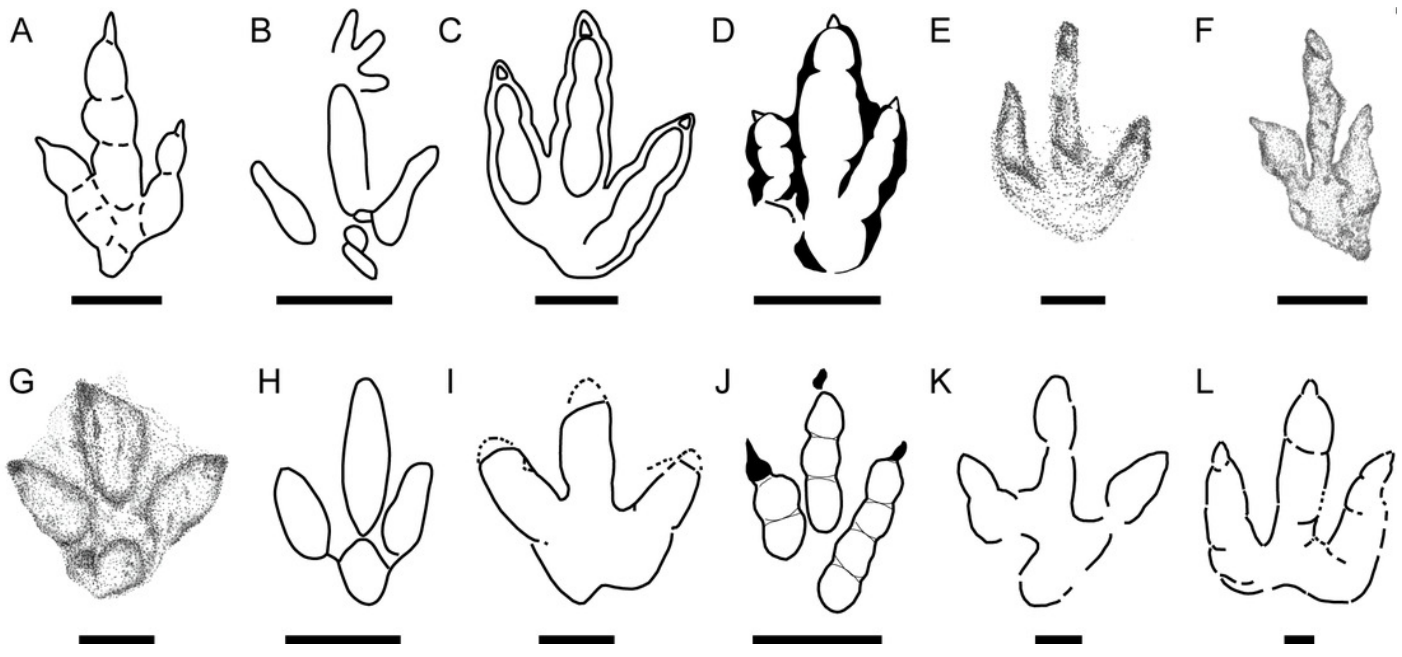

Figure 8

Small-medium-sized tridactyl dinosaur ichnotaxa with affinities with the described morphotypes.

A) Outline drawing of the holotype of *Carmelopodus untermannorum* (S, redrawn after Lockley et al., 1998b); B) Outline drawing of the holotype of *Wildeichnus navesi* (V, redrawn after Lockley, Mitchel & Odier, 2007); C) Outline drawing of the topotype of *Therangospodus pandemicus* (S, after Lockley, Meyer & Moratalla, 2000); D) Outline drawing of *Anomoepus scambus* (S, after Olsen & Rainforth, 2003); E) Outline drawing of the holotype of *Dineichnus socialis* (S, after Lockley et al., 1998a); F) Composite outline drawing of type trackway of *Grallator parallelus* (S, redrawn from Olsen, Smith & McDonald, 1998); G) Outline drawing of type specimen of *Anchisauripus sillimani* (S, redrawn from Olsen, Smith & McDonald, 1998); H) Outline drawing of type specimen of *Eubrontes giganteus* (S, redrawn from Olsen, Smith & McDonald, 1998). I) Outline drawing of type specimen of *Jialingpus yuechiensis* (S, redrawn from Lockley et al., 2013); J) Outline drawing of type specimen of *Kalohipus bretunensis* (S, redrawn from Fuentes Vidarte & Meijide Calvo, 1998). K) Outline drawing of type specimen of *Jurabrontes curtedulensis* (redrawn from Marty et al., 2017). L) Outline drawing of type specimen of *Megalosauripus transjuranicus* (redrawn from Razzolini et al., 2017). M) Outline drawing of specimen BSY1020-E2 (cf. *Kalohipus* isp.). N) Outline drawing of specimen CRO500-T10-L10 (cf. *Kalohipus* isp.). O) Outline drawing of specimen TCH-1060-E58 (cf. *Kalohipus* isp.); P) Outline drawing of specimen TCH-1065-T21-R1 (cf. *Therangospodus* isp.). Q) Outline drawing of specimen BEB500-T120-R5 (*Therangospodus*? isp.). S, C and V refer to siliciclastic, carbonate and volcanoclastic substrate, respectively. Scale bar = 2 cm (B, D), 5 cm (F,G, H, I, J), 10 cm (A, C, E, L, M-Q), 50 cm (K). Source credit: OCC-SAP, Canton Jura.

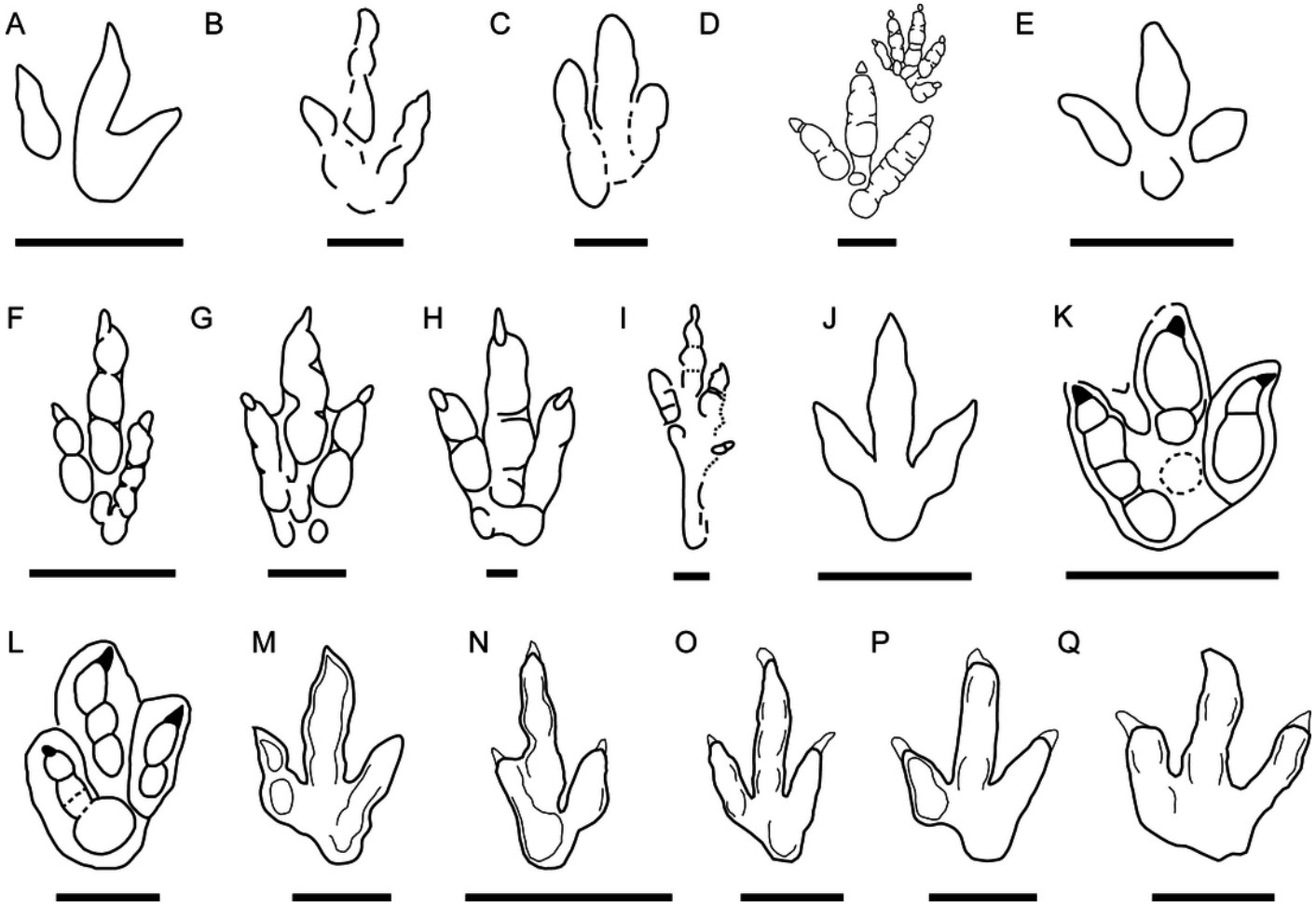
A
B
C
D
E
F
G
H
I
J
K
L
M
N
O
P
Q

Figure 9

Bivariate graph plotting the footprint length/footprint width ratio against AT of the studied tracks (gracile and robust morphotype) with some of the main dinosaur tridactyl of ichnotaxa mentioned in the text.

Outline drawings not to scale. Source credit: OCC-SAP, Canton Jura.

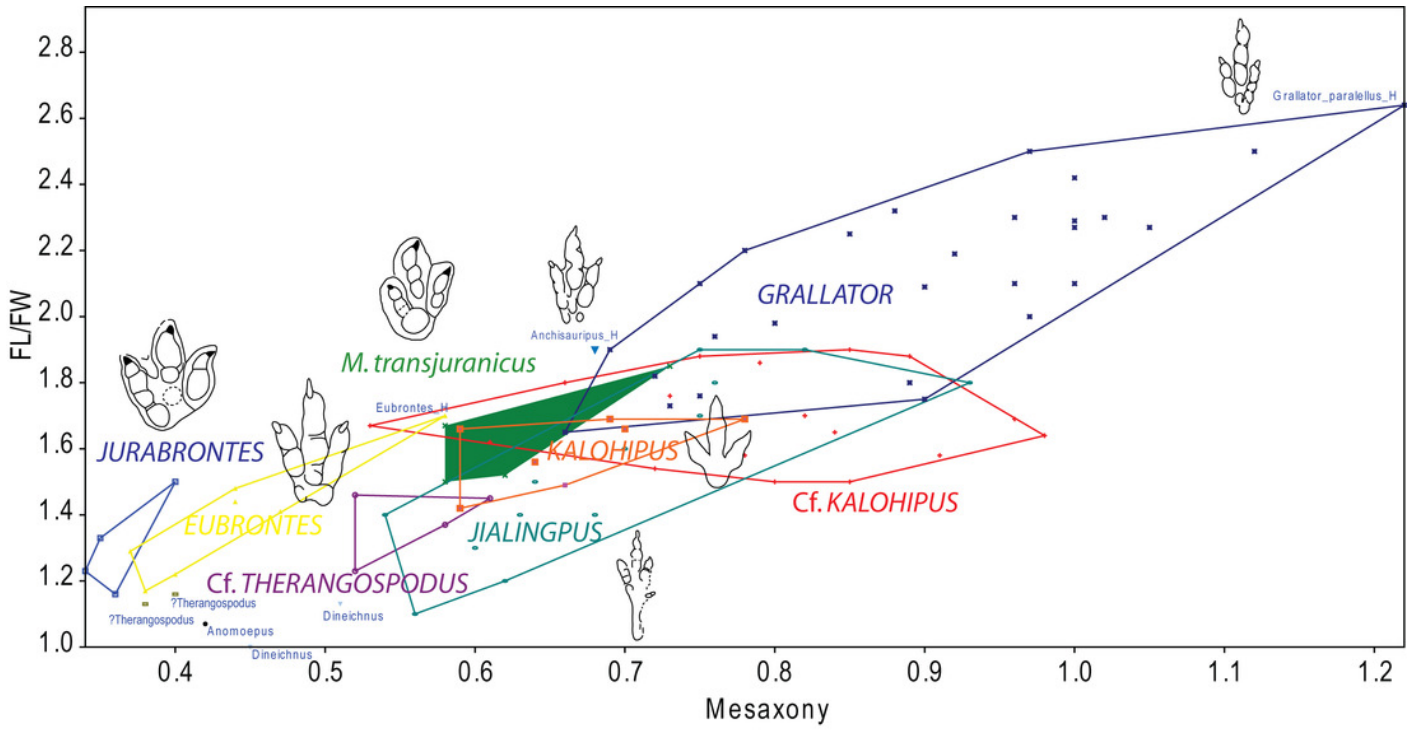

Table 1(on next page)

Measurements of the specimens with a high preservation grade:

footprint length (FL), footprint width (FW), footprint length /footprint width ratio (FL/FW), digit length (LI, LII, LIII), digit width (WI, WII, WIII), divarication angles (II-III, III-IV), mesaxony (AT, anterior triangle ratio; ATw, anterior triangle width; ATl, anterior triangle length).

Track	FL	FW	FL/FW	LII	LIII	LIV	WII	WIII	WIV	II^III	III^IV	ATw	Atl	AT
BEB500-T16-R3	18	10	1.8	13.5	18	13.8	2	1.9	1.8	22.5	17.5	8.8	5.8	0.66
BEB500-T17-R8	19	11.5	1.65	11	19	13	1.9	3.3	1.6	23	20	10.5	8.8	0.84
BEB500-T26-R5	19	12	1.58	13	19	14	2.2	3	2.9	32	26	10.3	9.4	0.91
BEB500-T73-L5	15	8.5	1.76	8.5	15	10	2.3	2.9	2.5	31	22	7.9	5.8	0.73
BSY1020-E2	22	11.7	1.88	15	22	13.5	3.6	3	2.7	21.5	24.5	9.5	8.5	0.89
TCH1055-E53	17.5	10.3	1.7	12.2	17.5	12	3	2.7	2.5	25	17.5	8.5	7	0.82
TCH1055-T2-L1	21.2	13.1	1.62	15.6	21.2	15	2.3	2.1	2.2	25	22	11.4	7	0.61
TCH1055-T2-R1	19.5	13	1.5	13.2	20.5	13.1	3.3	3.7	2.5	29	23	10.6	8.5	0.80
TCH1060-E58	20	10.5	1.90	20	13.5	12	3.4	3.1	2.9	27	22	8.8	7.5	0.85
TCH1065-E177	17.5	9.4	1.86	11.8	17.5	12.5	1.6	2.4	2	21	20	8.2	6.5	0.79
TCH1065-E3	18.4	12.3	1.5	12.3	18.4	11.7	3.3	3.8	2.3	30	24	9.14	7.8	0.85
TCH1065-T25-L2	19.3	12.2	1.58	14	19.3	12.3	3	3	2.7	25	21	10.3	8	0.78
TCH1069-T1-R2	20	13	1.54	14	20	13.5	2.1	2.7	2.1	24	29	11.5	8.3	0.72
SCR1055-T2-L2	20	12	1.67	15	20	16	2.7	2.9	2.5	25	18	11.4	6	0.53
SCR1055-T3-L2	18	11	1.64	12	18	12	2.3	2.1	1.8	26	26	8.5	8.3	0.98
CHV1000-E4	16	8.5	1.88	11	16	10	1.8	2.3	1.7	21	22	8.1	6.1	0.75
CRO500-T10-L10	11	6.5	1.69	6	11	7	1.4	1.8	1.5	32	23	5.6	5.4	0.96
BEB500-T120-R5	17	15	1.13	13.5	17	14.5	3.5	3.2	2.5	30.4	34	13	5	0.38
BEB500-T120-R6	18	15.5	1.16	14.5	18	15	2.5	3.1	3	22	27	14.2	5.7	0.40
TCH1065-E124	19	15.5	1.23	13.5	19	15	3.3	4.5	3.5	27.5	26.5	14.4	7.5	0.52
TCH1065-E188	18	12.3	1.46	13.3	18	13	3.2	3.7	3.3	25	27	10	5.2	0.52
TCH1065-T21-R1	19.8	14.5	1.37	14.4	19.8	14.8	3.5	3.7	3.5	27	27	11.8	6.9	0.58
TCH1065-T15-R1	21.8	15	1.45	15.7	21.8	17.2	2.7	3.4	3.1	29	25	12	7.3	0.61

Table 2 (on next page)

Variation in preservation grade and variation in maximum depth (difference between highest and lowest value) through the analysed trackways (see Table S1 for specific values of each track).

GRACILE MORPHOTYPE					ROBUST MORPHOTYPE				
Trackway	Number of tracks	Analysed tracks	Variation in preservation grade (min-max)	Total variation in depth(mm)	Trackway	Number of tracks	Analysed tracks	Variation in preservation grade (min-max)	Total variation in depth(mm)
BEB500-T16	27	3	0.5-2.5 (High)	1.1	BEB500-T75	71	2	0	0
BEB500-T17	120	4	1-2 (Medium)	2.8	BEB500-T120	29	4	0-2 (High)	5.8
BEB500-T58	53	6	0.5-1.5 (Medium)	2.3	TCH1065-T15	2	2	0.5-2 (High)	1.5
BEB500-T73	18	4	1-2 (Medium)	2	TCH1069-T2	5	2	1-1.5 (Low)	1.8
BEB500-T78	24	2	1-1 (Low)	0.4					
BEB500-T82	59	2	1.5-1.5 (Low)	1.9					
BEB500-T93	64	2	1-1.5 (Low)	3.8					
CRO500-T10	75	14	0-2 (High)	2.6					
CRO500-T30BIS	11	5	0-2 (High)	4.7					
TCH1055-T2	4	2	2-2.5 (Low)	2.5					
TCH1065-T25	4	2	1-2 (Medium)	2.7					

1